

Reduced density matrix functional theory from an *ab initio* seniority-zero wave function: Exact and approximate formulations along adiabatic connection paths

Bruno Senjean,^{1,*} Saad Yalouz,² Naoki Nakatani,^{3,4} and Emmanuel Fromager²

¹*ICGM, Université de Montpellier, CNRS, ENSCM, Montpellier, France*

²*Laboratoire de Chimie Quantique, Institut de Chimie,*

CNRS/Université de Strasbourg, 4 rue Blaise Pascal, 67000 Strasbourg, France

³*Department of Chemistry, Graduate School of Science and Engineering,*

Tokyo Metropolitan University, 1-1 Minami-Osawa, Hachioji, Tokyo 192-0397, Japan

⁴*Institute for Catalysis, Hokkaido University, N21W10 Kita-ku, Sapporo, Hokkaido 001-0021, Japan*

(Dated: August 15, 2022)

Currently, there is a growing interest in the development of a new hierarchy of methods based on the concept of seniority, which has been introduced quite recently in quantum chemistry. Despite the enormous potential of these methods, the accurate description of both dynamical and static correlation effects within a single and in-principle-exact approach remains a challenge. In this work, we propose an alternative formulation of reduced density-matrix functional theory (RDMFT) where the (one-electron reduced) density matrix is mapped onto an *ab initio* seniority-zero wave function. In this theory, the exact natural orbitals and their occupancies are determined self-consistently from an effective seniority-zero calculation. The latter involves a universal higher-seniority density matrix functional for which an adiabatic connection (AC) formula is derived and implemented under specific constraints that are related to the density matrix. The pronounced curvature of the (constrained) AC integrand, which is numerically observed in prototypical hydrogen chains and the Helium dimer, indicates that a description of higher-seniority correlations within second-order perturbation theory is inadequate in this context. Applying multiple linear interpolations along the AC or connecting second-order perturbation theory to a full-seniority treatment *via* Padé approximants are better strategies. Such information is expected to serve as a guide in the future design of higher-seniority density-matrix functional approximations.

I. INTRODUCTION

The accurate description of chemical compounds which manifest both weak and strong correlation effects (also referred to as dynamical and static correlation effects, respectively [1, 2]) remains a long-standing challenge in the quantum chemistry community. One angle of attack to tackle the electronic structure problem is to construct orbital-based wave functions, expressed as linear combination of Slater determinants. Most quantum chemistry methods are built upon Hartree–Fock (HF) theory and include corrections from excited-state configurations, thus leading to configuration interaction (CI) and coupled cluster (CC) methods [3]. If all configurations are considered, it is called the full configuration interaction (FCI) and all the correlation effects are captured. Unfortunately, the computational cost associated to FCI scales exponentially with the system size, such that the configuration space is commonly truncated to single and double excited-state configurations (CISD and CCSD). Despite the success of those approximations (CC is considered as the “gold standard” method in quantum chemistry [4, 5]), strong correlation effects are still insufficiently described. A similar conclusion holds for the Kohn–Sham density functional theory (KS-DFT) [6, 7] whose density functional approximations are not able to describe strong correlation effects [8–10]. Instead of using

the electronic density as a basic variable, one can consider the one-particle reduced density matrix (1RDM), thus leading to the reduced density matrix functional theory (RDMFT) [11–14]. Several 1RDM functionals based on the occupation numbers of the natural orbitals have been developed [15–24], in particular the Piris natural orbital functionals PNOF i ($i = 1, 7$) [25–36]. In order to treat both the static and dynamical correlations simultaneously, several hybrid schemes, where wave function theory is combined with the aforementioned reduced quantity theories [37–47], have been proposed. Quite recently, Pernal [48] also suggested to use the adiabatic connection (AC) formalism to recover the electron correlation that is missing in multiconfigurational wave functions [49–52].

Post-HF methods are adequate for treating weakly correlated systems. When it comes to describing strongly correlated systems, a more appealing strategy consists in dropping the orbital picture and, instead, constructing wave functions as products of geminals (*i.e.*, pairs of electrons) [53–61]. A hierarchy of these methods can be found in Ref. [62]. Starting from the idea of pairing electrons, one can divide the entire many-electron Hilbert space into subspaces by using the concept of seniority number. The latter corresponds to the number of unpaired electrons in a determinant [63, 64]. If all electrons are paired (*i.e.*, all spatial orbitals are either doubly occupied or unoccupied), the wave function is referred to as *seniority-zero* wave function. It is described exactly by performing a doubly occupied configuration interaction (DOCI) calculation [65] where

* Corresponding author; bruno.senjean@umontpellier.fr

the seniority-zero part of the Hamiltonian [66] is diagonalized.

Even though seniority-zero wave functions can describe accurately strong (static) correlation effects, their evaluation is computationally demanding and a proper description of dynamical correlation effects requires taking into account higher seniorities [67] or mixing excitation degrees and seniority numbers [68]. Other promising approaches that retain the computational cost of a mean-field and are adequate for the treatment of strong correlation have been proposed, like the so-called antisymmetric product of one-reference-orbital geminals (AP1roG) [62, 69–71] equivalent to the pair-coupled cluster theory (pCCD) [72, 73], or more recently the pair parametric two-electron reduced density matrix approach [74]. Open-shell extensions of pCCD have also been developed in Ref. 75. Orbital optimization is essential in these approaches for the accurate description of both ground [71, 72, 76–78] and excited states [79–82]. Despite promising results, AP1roG and related geminal-based wave functions are not adequate to capture dynamical correlation [83]. Indeed, dynamical correlation is not described by electron-pair states but by higher-seniority contributions. The latter can be determined from perturbation theory [84–94], coupled-cluster theory [94–102], the extended random phase approximation [103, 104], DFT [105–107], or the AC formalism [108]. In the spirit of post-HF methods, post-Antisymmetrized Geminal Power approaches are also promising, not only on classical computers [109–112], but also on quantum computers [113].

In this work, we propose to formally exactify seniority-zero wave function calculations in the context of *reduced density matrix functional theory* (RDMFT). More precisely, by analogy with KS-DFT, we will map the 1RDM onto a reference *ab initio* seniority-zero wave function. In this context, the higher-seniority correlation effects will be described by a density matrix functional. The paper is organized as follows. In Sec. II, we present an exact reformulation of RDMFT as an effective seniority-zero theory. The self-consistent calculation of both the natural orbitals and their occupancies will be discussed in this context. In order to give further insight into the complementary higher-seniority density-matrix correlation functional, which is a central object in the theory, two different adiabatic connection paths are constructed in Sec. III. Details about the computational implementation of the adiabatic connections are provided in Sec. IV, which is followed by a detailed discussion in Sec. V of the results obtained for the prototypical H_4 and H_8 chains, as well as the Helium dimer. Conclusions and perspectives are given in Sec. VI.

II. THEORY

A. Seniority-zero wave function and Hamiltonian

The concept of seniority has been introduced recently in quantum chemistry by Scuseria and co-workers [63]. It consists in partitioning the FCI Fock space into subspaces that are defined from the following seniority number operator:

$$\hat{\Omega} = \sum_p (\hat{n}_{p\uparrow} + \hat{n}_{p\downarrow} - 2\hat{n}_{p\uparrow}\hat{n}_{p\downarrow}), \quad (1)$$

where $\hat{n}_{p\sigma} \equiv \hat{c}_{p\sigma}^\dagger \hat{c}_{p\sigma}$ [$\sigma = \uparrow, \downarrow$] is a spin-orbital occupation operator written in second quantization. As readily seen from Eq. (1), the seniority operator $\hat{\Omega}$ simply counts the number of unpaired electrons in a given configuration. It has been shown that the seniority-zero sector, which is denoted S_0 in the following and for which $\langle \hat{\Omega} \rangle_{S_0} = 0$, contributes significantly to the description of static correlation [63]. In the DOCI approximation [65], FCI is applied to the seniority-zero subspace, which means that determinants with empty or doubly occupied orbitals only are considered in the calculation. In such a case, the wave function ansatz reads

$$S_0 \ni \Psi \equiv \sum_{p_1 < \dots < p_{N/2}} C_{p_1 \dots p_{N/2}} \prod_{i=1}^{N/2} \hat{c}_{p_i \uparrow}^\dagger \hat{c}_{p_i \downarrow}^\dagger |\text{vac}\rangle, \quad (2)$$

where $|\text{vac}\rangle$ denotes the vacuum state and N is the (even) number of electrons. Note that the 1RDM of a seniority-zero wave function is diagonal in its orbital basis:

$$D_{pq}^\Psi = \sum_{\sigma} \langle \Psi | \hat{c}_{p\sigma}^\dagger \hat{c}_{q\sigma} | \Psi \rangle \stackrel{\Psi \in S_0}{=} \delta_{pq} n_p^\Psi, \quad (3)$$

where

$$n_p^\Psi = 2 \sum_{p_1 < \dots < p_{N/2}} |C_{p_1 \dots p_{N/2}}|^2 \sum_{i=1}^{N/2} \delta_{pp_i}. \quad (4)$$

In other words, these orbitals are the seniority-zero natural orbitals, by construction. By analogy with the *multiconfigurational self-consistent field* (MCSCF) method [3], they can be optimized variationally, in addition to the DOCI coefficients $\{C_{p_1 \dots p_{N/2}}\}$ [108]. In the present work, we aim at deriving an in-principle-exact variational energy expression such that the minimizing seniority-zero orbitals match the exact natural orbitals of the true (higher-seniority) physical many-body wave function. As briefly sketched in the following and further formalized in the next subsections, we need for that purpose to introduce a density matrix functional correction to the (approximate) seniority-zero energy.

Let us start with the general (*ab initio*) second-

quantized Hamiltonian expression,

$$\hat{H} = \sum_{pq} \sum_{\sigma} h_{pq} \hat{c}_{p\sigma}^{\dagger} \hat{c}_{q\sigma} + \hat{W}_{ee}, \quad (5)$$

$$\hat{W}_{ee} = \frac{1}{2} \sum_{pqrs} \langle pq|rs \rangle \sum_{\sigma\sigma'} \hat{c}_{p\sigma}^{\dagger} \hat{c}_{q\sigma'}^{\dagger} \hat{c}_{s\sigma'} \hat{c}_{r\sigma}, \quad (6)$$

where $h_{pq} = \langle \varphi_p | \hat{h} | \varphi_q \rangle = \int d\mathbf{r} \varphi_p(\mathbf{r}) \left[-\frac{1}{2} \nabla_{\mathbf{r}}^2 + v_{ne}(\mathbf{r}) \right] \varphi_q(\mathbf{r})$ and $\langle pq|rs \rangle = \int \int d\mathbf{r} d\mathbf{r}' \varphi_p(\mathbf{r}) \varphi_q(\mathbf{r}') \varphi_r(\mathbf{r}) \varphi_s(\mathbf{r}') / |\mathbf{r} - \mathbf{r}'|$ are the one-electron (kinetic and nuclear potential energies) and two-electron repulsion integrals, respectively. The DOCI Hamiltonian, that we refer to as seniority-zero Hamiltonian in the following, is obtained simply by removing all but the terms that preserve the seniority-zero character of the trial wave function in Eq. (2). As a result, the one-electron Hamiltonian reduces to its diagonal part while only two orbitals (that may be identical) should remain in the two-electron repulsion operator:

$$\hat{H} \rightarrow \hat{H}^{S_0} = \sum_p h_{pp} \hat{n}_p + \hat{W}_{ee}^{S_0}, \quad (7)$$

where

$$\begin{aligned} \hat{W}_{ee}^{S_0} &= \sum_{p>q} \langle pq|pq \rangle \hat{n}_p \hat{n}_q - \sum_{p>q} \sum_{\sigma} \langle pq|qp \rangle \hat{n}_{p\sigma} \hat{n}_{q\sigma} \\ &+ \sum_{pq} \langle pp|qq \rangle \hat{P}_p^{\dagger} \hat{P}_q, \end{aligned} \quad (8)$$

$\hat{n}_p = \hat{n}_{p\uparrow} + \hat{n}_{p\downarrow}$, and $\hat{P}_p^{\dagger} = \hat{c}_{p\uparrow}^{\dagger} \hat{c}_{p\downarrow}^{\dagger}$ is the creation operator of a pair of electrons in the p th orbital. Interestingly, we recognize in the seniority-zero interaction operator the direct $\mathcal{J}_{pq} = \langle pq|pq \rangle$, exchange $\mathcal{K}_{pq} = \langle pq|qp \rangle$, and exchange-time-inversion $\mathcal{L}_{pq} = \langle pp|qq \rangle$ integrals which are central in the implementation of the Piris natural orbital functionals [32, 93]. Note that, in the present work, we use real algebra and therefore $\mathcal{L}_{pq} = \mathcal{K}_{pq}$. In addition, unlike in Ref. 66, we do not proceed in Eq. (8) with the simplification $\hat{n}_{p\uparrow} \equiv \hat{n}_{p\downarrow} \equiv \hat{n}_p/2$, which holds on the seniority-zero subspace. This is only for convenience, as we will implement later on an adiabatic connection path between the (approximate) seniority-zero and exact (higher-seniority) Hamiltonians [see Sec. III A].

For two-electron systems in the ground state, \hat{H}^{S_0} becomes exact if written in the exact natural orbital basis. In this particular case, the seniority-zero wave function is the Löwdin–Shull one [114, 115]. In the general case, \hat{H}^{S_0} is an approximation to the true Hamiltonian \hat{H} . Nevertheless, the seniority-zero picture may become *exact*, in the spirit of KS-DFT, if it reproduces the true physical (with all higher seniorities included) 1RDM. As readily seen from Eq. (3), it immediately implies that the seniority-zero and true natural orbitals should match. In addition, the to-be-determined fictitious seniority-zero wave function Ψ^{S_0} should reproduce the natural orbital

occupations of the true physical ground-state wave function Ψ_0 :

$$n_p^{\Psi^{S_0}} = n_p^{\Psi_0}. \quad (9)$$

By analogy with DFT for lattice models [116], we can impose the orbital occupation constraint of Eq. (9) [which can be seen as a density constraint in the natural orbital space] by adjusting the one-electron energies,

$$h_{pp} \rightarrow h_{pp} + \bar{\varepsilon}_p, \quad (10)$$

thus leading to the following seniority-zero Schrödinger-like equation:

$$\left[\sum_p (h_{pp} + \bar{\varepsilon}_p) \hat{n}_p + \hat{W}_{ee}^{S_0} \right] |\Psi^{S_0}\rangle = \mathcal{E}^{S_0} |\Psi^{S_0}\rangle, \quad (11)$$

where $\{h_{pp} + \bar{\varepsilon}_p\}$, which is unique up to a constant, can be seen as the analog (in the natural orbital space) of the KS potential for seniority-zero wave functions. Note that the extension of the Hohenberg–Kohn theorem to lattice Hamiltonians holds also in this context (see Appendix A). If we compare with the KS Hamiltonian for Hubbard [116], the one-electron hopping operator (which is a model for the kinetic energy operator) is now replaced by the two-electron seniority-zero repulsion operator $\hat{W}_{ee}^{S_0}$. The annihilation-creation of electron pairs [third term on the right-hand side of Eq. (8)] delocalizes the electrons in the natural orbital space, thus ensuring that all DOCI coefficients are in principle non-zero. This observation becomes central when establishing a one-to-one correspondence between $\{h_{pp} + \bar{\varepsilon}_p\}$, that we simply refer to as *potential* in the following, and the ground-state seniority-zero wave function.

In the rest of this work we will show how the natural orbitals and the potential $\{\bar{\varepsilon}_p\}$ can be determined, in principle exactly, from a universal density matrix functional. This functional enables the exact evaluation of the true ground-state energy from the fictitious seniority-zero wave function Ψ^{S_0} .

B. Natural orbital functional theory and orbital rotations

In RDMFT [11], the exact ground-state energy can in principle be obtained variationally as follows,

$$E = \min_{\mathbf{D}} \left\{ \text{Tr} [\mathbf{h}\mathbf{D}] + W(\mathbf{D}) \right\}, \quad (12)$$

where Tr denotes the trace, $\mathbf{h} \equiv \{h_{pq}\}$ is the one-electron (kinetic and nuclear potential) Hamiltonian matrix, and $\mathbf{D} \equiv \{D_{pq}\}$ is a trial (spin-summed) N -representable 1RDM. For simplicity, 1RDMs will simply be referred to as *density matrices* in the following. Within Levy's constrained-search formalism [117], the interaction energy functional reads

$$W(\mathbf{D}) = \min_{\Psi \rightarrow \mathbf{D}} \langle \Psi | \hat{W}_{ee} | \Psi \rangle. \quad (13)$$

Like in *natural orbital functional theory* (NOFT) [33], we adopt the natural orbital representation of the density matrix in the rest of this work. Moreover, for convenience, we will use an exponential parameterization of the natural orbitals, like in the MCSCF method [3]. Let $\{\varphi_p(\mathbf{r})\}$ be an arbitrary (orthonormal) molecular orbital basis. Any natural orbital basis can be obtained from the latter by rotation,

$$\varphi_p(\mathbf{r}) \rightarrow \varphi_{p(\boldsymbol{\kappa})}(\mathbf{r}) = \sum_q [e^{-\boldsymbol{\kappa}}]_{qp} \varphi_q(\mathbf{r}), \quad (14)$$

where $\boldsymbol{\kappa} = -\boldsymbol{\kappa}^\dagger \equiv \{\kappa_{pq}\}_{p>q}$. Note that, in second quantization, Eq. (14) can be reformulated as follows [3],

$$\hat{c}_{p(\boldsymbol{\kappa})\sigma}^\dagger = e^{-\hat{\kappa}} \hat{c}_{p\sigma}^\dagger e^{\hat{\kappa}}, \quad (15)$$

where $\hat{\kappa} = \sum_{p>q} \kappa_{pq} \sum_\sigma (\hat{c}_{p\sigma}^\dagger \hat{c}_{q\sigma} - \hat{c}_{q\sigma}^\dagger \hat{c}_{p\sigma})$ is the real antihermitian singlet rotation operator. The interaction functional in Eq. (13) can now be rewritten as follows:

$$\begin{aligned} W(\mathbf{D} \equiv (\boldsymbol{\kappa}, \mathbf{n})) &= \min_{\Psi \rightarrow (\boldsymbol{\kappa}, \mathbf{n})} \langle \Psi | \hat{W}_{ee} | \Psi \rangle \\ &= \langle \hat{W}_{ee} \rangle_{\Psi(\boldsymbol{\kappa}, \mathbf{n})}, \end{aligned} \quad (16)$$

where $\mathbf{n} \equiv \{n_p\}$ are the natural orbital occupancies and the constraint $\Psi \rightarrow (\boldsymbol{\kappa}, \mathbf{n})$, which reads

$$\begin{aligned} \sum_\sigma \langle \Psi | \hat{c}_{p(\boldsymbol{\kappa})\sigma}^\dagger \hat{c}_{q(\boldsymbol{\kappa})\sigma} | \Psi \rangle &= n_p \delta_{p(\boldsymbol{\kappa})q(\boldsymbol{\kappa})} \\ \stackrel{\text{notation}}{\Leftrightarrow} \Psi &\longrightarrow \text{diag}[\mathbf{n}], \\ &\{\varphi_{p(\boldsymbol{\kappa})}\} \end{aligned} \quad (17)$$

means that the rotated orbitals $\{\varphi_{p(\boldsymbol{\kappa})}\}$ are the natural orbitals of Ψ (with occupations \mathbf{n}). In the light of Eq. (17), it seems relevant (but it is not compulsory) to expand the minimizing wave function of Eq. (16) in the rotated orbital basis:

$$|\Psi(\boldsymbol{\kappa}, \mathbf{n})\rangle \equiv \sum_I C_I(\boldsymbol{\kappa}, \mathbf{n}) |\Phi_I(\boldsymbol{\kappa})\rangle, \quad (18)$$

where $|\Phi_I(\boldsymbol{\kappa})\rangle$ is a ‘‘rotated’’ Slater determinant (*i.e.*, it is constructed from the rotated orbitals $\{\varphi_{p(\boldsymbol{\kappa})}\}$). Note that, according to Eq. (15), rotated determinants are connected to the unrotated ones $\Phi_I \equiv \Phi_I(\boldsymbol{\kappa} = 0)$ as follows,

$$|\Phi_I(\boldsymbol{\kappa})\rangle = e^{-\hat{\kappa}} |\Phi_I\rangle. \quad (19)$$

We should also stress that, unlike its seniority-zero approximation, the full two-electron repulsion operator in Eq. (6) is invariant under orbital rotation, *i.e.*,

$$2\hat{W}_{ee} = \sum_{pqrs} \langle pq|rs \rangle^\kappa \sum_{\sigma\sigma'} \hat{c}_{p(\boldsymbol{\kappa})\sigma}^\dagger \hat{c}_{q(\boldsymbol{\kappa})\sigma'}^\dagger \hat{c}_{s(\boldsymbol{\kappa})\sigma'} \hat{c}_{r(\boldsymbol{\kappa})\sigma} \quad (20)$$

where $\langle pq|rs \rangle^\kappa = \langle p(\boldsymbol{\kappa})q(\boldsymbol{\kappa})|r(\boldsymbol{\kappa})s(\boldsymbol{\kappa}) \rangle$ are the two-electron integrals evaluated from the rotated orbitals.

For reasons that will become clearer in the following, we now proceed with a *picture change* in Eq. (16):

$$\Psi \rightarrow \tilde{\Psi} = e^{+\hat{\kappa}} \Psi, \quad (21)$$

where the rotation operator $\hat{\kappa}$ is constructed from the $\boldsymbol{\kappa}$ matrix [see below Eq. (15)] which is *fixed* when evaluating the interaction functional of Eq. (16). When applied to the minimizing wave function, the picture change gives [see Eq. (19)]

$$e^{+\hat{\kappa}} |\Psi(\boldsymbol{\kappa}, \mathbf{n})\rangle \equiv \sum_I C_I(\boldsymbol{\kappa}, \mathbf{n}) |\Phi_I\rangle. \quad (22)$$

Therefore, in the new picture, the correct CI coefficients $C_I(\boldsymbol{\kappa}, \mathbf{n})$ are used in the (incorrect) unrotated natural orbital basis. The formal advantage is that trial wave functions can now be expanded in the (arbitrary and) fixed orbital basis $\{\varphi_p\}$. Obviously, we now need to employ picture-changed operators. For example,

$$\langle \Psi | \hat{W}_{ee} | \Psi \rangle = \langle \tilde{\Psi} | \hat{W}_{ee}(\boldsymbol{\kappa}) | \tilde{\Psi} \rangle, \quad (23)$$

where the full (natural orbital-dependent) picture-changed two-electron interaction operator $\hat{W}_{ee}(\boldsymbol{\kappa})$ reads, according to Eqs. (15) and (21), and the expression of \hat{W}_{ee} in Eq. (20),

$$\begin{aligned} \hat{W}_{ee}(\boldsymbol{\kappa}) &= e^{+\hat{\kappa}} \hat{W}_{ee} e^{-\hat{\kappa}} \\ &= \frac{1}{2} \sum_{pqrs} \langle pq|rs \rangle^\kappa \sum_{\sigma\sigma'} \hat{c}_{p\sigma}^\dagger \hat{c}_{q\sigma'}^\dagger \hat{c}_{s\sigma'} \hat{c}_{r\sigma}. \end{aligned} \quad (24)$$

Note that $\hat{W}_{ee}(\boldsymbol{\kappa})$ is expressed in terms of the unrotated creation/annihilation operators because, according to Eq. (15), $e^{+\hat{\kappa}} \hat{c}_{p(\boldsymbol{\kappa})\sigma}^\dagger e^{-\hat{\kappa}} = \hat{c}_{p\sigma}^\dagger$. Finally, since

$$\delta_{p(\boldsymbol{\kappa})q(\boldsymbol{\kappa})} = \langle \varphi_{p(\boldsymbol{\kappa})} | \varphi_{q(\boldsymbol{\kappa})} \rangle = \langle \varphi_p | \varphi_q \rangle = \delta_{pq}, \quad (25)$$

according to Eq. (14), the constraint in Eq. (17) becomes in the new picture [see Eqs. (15) and (21)],

$$\begin{aligned} \sum_\sigma \langle \tilde{\Psi} | \hat{c}_{p\sigma}^\dagger \hat{c}_{q\sigma} | \tilde{\Psi} \rangle &= n_p \delta_{pq} \\ \stackrel{\text{notation}}{\Leftrightarrow} \tilde{\Psi} &\rightarrow \text{diag}[\mathbf{n}], \end{aligned} \quad (26)$$

which means that the unrotated orbitals should be the natural orbitals of the trial wave function $\tilde{\Psi}$ (with occupations \mathbf{n}).

To conclude, if we employ the picture change of Eq. (21), the universal interaction density matrix functional of Eq. (16) can be rewritten as follows [see Eqs. (23) and (26)],

$$W(\boldsymbol{\kappa}, \mathbf{n}) = \min_{\tilde{\Psi} \rightarrow \text{diag}[\mathbf{n}]} \langle \tilde{\Psi} | \hat{W}_{ee}(\boldsymbol{\kappa}) | \tilde{\Psi} \rangle. \quad (27)$$

We will use the above expression for introducing seniority-zero wave functions in RDMFT.

C. Seniority-zero interaction density matrix functional

On the basis of Eq. (27), we define the seniority-zero analog of the interaction functional as follows,

$$W^{\mathcal{S}_0}(\boldsymbol{\kappa}, \mathbf{n}) = \min_{\tilde{\Psi} \rightarrow \text{diag}[\mathbf{n}]} \left\langle \tilde{\Psi} \left| \hat{W}_{\text{ee}}^{\mathcal{S}_0}(\boldsymbol{\kappa}) \right| \tilde{\Psi} \right\rangle, \quad (28)$$

where, in analogy with Eq. (8), all but the seniority-zero components have been removed from the two-electron repulsion operator $\hat{W}_{\text{ee}}(\boldsymbol{\kappa})$:

$$\begin{aligned} \hat{W}_{\text{ee}}^{\mathcal{S}_0}(\boldsymbol{\kappa}) &= \sum_{p>q} \langle pq|pq \rangle^{\boldsymbol{\kappa}} \hat{n}_p \hat{n}_q - \sum_{p>q} \sum_{\sigma} \langle pq|qp \rangle^{\boldsymbol{\kappa}} \hat{n}_{p\sigma} \hat{n}_{q\sigma} \\ &+ \sum_{pq} \langle pp|qq \rangle^{\boldsymbol{\kappa}} \hat{P}_p^\dagger \hat{P}_q. \end{aligned} \quad (29)$$

Let us now introduce, in the light of Sec. II A, the ground-state wave function $\Psi^{\mathcal{S}_0}(\boldsymbol{\kappa}, \mathbf{n})$ of the seniority-zero Hamiltonian $\hat{W}_{\text{ee}}^{\mathcal{S}_0}(\boldsymbol{\kappa}) + \sum_p \varepsilon_p(\boldsymbol{\kappa}, \mathbf{n}) \hat{n}_p$ with natural orbital occupations \mathbf{n} . For *any* wave function Ψ fulfilling the (not necessarily natural) orbital occupation constraint

$$\{\langle \Psi | \hat{n}_p | \Psi \rangle\} = \mathbf{n}, \quad (30)$$

that we simply denote $\Psi \rightarrow \mathbf{n}$, we have, according to the variational principle,

$$\begin{aligned} &\langle \Psi^{\mathcal{S}_0}(\boldsymbol{\kappa}, \mathbf{n}) | \hat{W}_{\text{ee}}^{\mathcal{S}_0}(\boldsymbol{\kappa}) + \sum_p \varepsilon_p(\boldsymbol{\kappa}, \mathbf{n}) \hat{n}_p | \Psi^{\mathcal{S}_0}(\boldsymbol{\kappa}, \mathbf{n}) \rangle \\ &\leq \langle \Psi | \hat{W}_{\text{ee}}^{\mathcal{S}_0}(\boldsymbol{\kappa}) + \sum_p \varepsilon_p(\boldsymbol{\kappa}, \mathbf{n}) \hat{n}_p | \Psi \rangle, \end{aligned} \quad (31)$$

thus leading to

$$\langle \Psi^{\mathcal{S}_0}(\boldsymbol{\kappa}, \mathbf{n}) | \hat{W}_{\text{ee}}^{\mathcal{S}_0}(\boldsymbol{\kappa}) | \Psi^{\mathcal{S}_0}(\boldsymbol{\kappa}, \mathbf{n}) \rangle \leq_{\Psi \rightarrow \mathbf{n}} \langle \Psi | \hat{W}_{\text{ee}}^{\mathcal{S}_0}(\boldsymbol{\kappa}) | \Psi \rangle. \quad (32)$$

As a result, the density matrix constraint in the minimization of Eq. (28), which is obviously fulfilled by $\Psi^{\mathcal{S}_0}(\boldsymbol{\kappa}, \mathbf{n})$, can be relaxed, thus becoming the orbital occupation constraint of Eq. (30). This leads to the final Levy's constrained-search expression for the seniority-zero interaction energy functional:

$$\begin{aligned} W^{\mathcal{S}_0}(\boldsymbol{\kappa}, \mathbf{n}) &= \min_{\Psi \rightarrow \mathbf{n}} \langle \Psi | \hat{W}_{\text{ee}}^{\mathcal{S}_0}(\boldsymbol{\kappa}) | \Psi \rangle \\ &= \langle \Psi^{\mathcal{S}_0}(\boldsymbol{\kappa}, \mathbf{n}) | \hat{W}_{\text{ee}}^{\mathcal{S}_0}(\boldsymbol{\kappa}) | \Psi^{\mathcal{S}_0}(\boldsymbol{\kappa}, \mathbf{n}) \rangle. \end{aligned} \quad (33)$$

As the orbital occupation constraint is analogous to a density constraint on a lattice [116, 118], we can use convenient tools from DFT such as the Lieb maximization [118, 119] in order to evaluate the functional. Indeed, for *any* "potential" $\boldsymbol{\varepsilon} \equiv \{\varepsilon_p\}$, applying the variational principle to the seniority-zero Hamiltonian $\hat{W}_{\text{ee}}^{\mathcal{S}_0}(\boldsymbol{\kappa}) + \sum_p \varepsilon_p \hat{n}_p$ with ground-state energy $\mathcal{E}^{\mathcal{S}_0}(\boldsymbol{\kappa}, \boldsymbol{\varepsilon})$ gives

$$\begin{aligned} &\mathcal{E}^{\mathcal{S}_0}(\boldsymbol{\kappa}, \boldsymbol{\varepsilon}) \\ &\leq \langle \Psi^{\mathcal{S}_0}(\boldsymbol{\kappa}, \mathbf{n}) | \hat{W}_{\text{ee}}^{\mathcal{S}_0}(\boldsymbol{\kappa}) + \sum_p \varepsilon_p \hat{n}_p | \Psi^{\mathcal{S}_0}(\boldsymbol{\kappa}, \mathbf{n}) \rangle, \end{aligned} \quad (35)$$

thus leading to the alternative expression [see Eqs. (30) and (34)]

$$W^{\mathcal{S}_0}(\boldsymbol{\kappa}, \mathbf{n}) = \max_{\boldsymbol{\varepsilon}} \{ \mathcal{E}^{\mathcal{S}_0}(\boldsymbol{\kappa}, \boldsymbol{\varepsilon}) - \langle \boldsymbol{\varepsilon} | \mathbf{n} \rangle \}, \quad (36)$$

where $\langle \boldsymbol{\varepsilon} | \mathbf{n} \rangle = \sum_p \varepsilon_p n_p$. The practical implementation of Eq. (36) will be discussed further in Secs. IV and V.

Finally, we would like to emphasize that, even though the orbital occupation constraint of Eq. (30) is written, for convenience, in an arbitrary and fixed (unrotated) orbital basis, the seniority-zero interaction functional is a *universal* functional of the density matrix. In other words, unlike in DFT for lattice Hamiltonians [116], the (natural, in the present context) orbital basis on which the theory relies (through its dependence in $\boldsymbol{\kappa}$) is an additional basic variable that has to be optimized for a given system, exactly like in NOFT. This point can be further highlighted by making the dependence of the functional on the natural orbitals more explicit. Indeed, since $e^{-\hat{\kappa}} \Psi^{\mathcal{S}_0}(\boldsymbol{\kappa}, \mathbf{n})$ is the ground state of [see Eqs. (15) and (31)]

$$\begin{aligned} &e^{-\hat{\kappa}} \left(\hat{W}_{\text{ee}}^{\mathcal{S}_0}(\boldsymbol{\kappa}) + \sum_p \varepsilon_p(\boldsymbol{\kappa}, \mathbf{n}) \hat{n}_p \right) e^{\hat{\kappa}} \\ &= \sum_{p>q} \langle pq|pq \rangle^{\boldsymbol{\kappa}} \hat{n}_{p(\boldsymbol{\kappa})} \hat{n}_{q(\boldsymbol{\kappa})} \\ &- \sum_{p>q} \sum_{\sigma} \langle pq|qp \rangle^{\boldsymbol{\kappa}} \hat{n}_{p(\boldsymbol{\kappa})\sigma} \hat{n}_{q(\boldsymbol{\kappa})\sigma} \\ &+ \sum_{pq} \langle pp|qq \rangle^{\boldsymbol{\kappa}} \hat{P}_{p(\boldsymbol{\kappa})}^\dagger \hat{P}_{q(\boldsymbol{\kappa})} + \sum_p \varepsilon_p(\boldsymbol{\kappa}, \mathbf{n}) \hat{n}_{p(\boldsymbol{\kappa})}, \end{aligned} \quad (37)$$

with occupation numbers in the rotated basis [see Eq. (30)]

$$\begin{aligned} &\{ \langle e^{-\hat{\kappa}} \Psi^{\mathcal{S}_0}(\boldsymbol{\kappa}, \mathbf{n}) | \hat{n}_{p(\boldsymbol{\kappa})} | e^{-\hat{\kappa}} \Psi^{\mathcal{S}_0}(\boldsymbol{\kappa}, \mathbf{n}) \rangle \} \\ &= \{ \langle \Psi^{\mathcal{S}_0}(\boldsymbol{\kappa}, \mathbf{n}) | \hat{n}_p | \Psi^{\mathcal{S}_0}(\boldsymbol{\kappa}, \mathbf{n}) \rangle \} \\ &\equiv \mathbf{n}, \end{aligned} \quad (38)$$

it may be denoted as

$$e^{-\hat{\kappa}} \Psi^{\mathcal{S}_0}(\boldsymbol{\kappa}, \mathbf{n}) \equiv \overline{\Psi}^{\mathcal{S}_0}(\{ \varphi_{p(\boldsymbol{\kappa})} \}, \mathbf{n}) \quad (39)$$

and described as the (*ab initio*) seniority-zero analog of the ground-state wave function, both being written in the same basis of natural orbitals $\{ \varphi_{p(\boldsymbol{\kappa})} \}$ with occupations \mathbf{n} . As the seniority-zero Hamiltonian of Eq. (37) is a universal functional of the density matrix, so are $\overline{\Psi}^{\mathcal{S}_0}(\{ \varphi_{p(\boldsymbol{\kappa})} \}, \mathbf{n})$ and the resulting seniority-zero interaction functional [see Eq. (34)]:

$$\begin{aligned} &W^{\mathcal{S}_0}(\boldsymbol{\kappa}, \mathbf{n}) \\ &= \left\langle \overline{\Psi}^{\mathcal{S}_0}(\{ \varphi_{p(\boldsymbol{\kappa})} \}, \mathbf{n}) \left| e^{-\hat{\kappa}} \hat{W}_{\text{ee}}^{\mathcal{S}_0}(\boldsymbol{\kappa}) e^{\hat{\kappa}} \right| \overline{\Psi}^{\mathcal{S}_0}(\{ \varphi_{p(\boldsymbol{\kappa})} \}, \mathbf{n}) \right\rangle \\ &= \left\langle \overline{\Psi}^{\mathcal{S}_0}(\{ \varphi_{p(\boldsymbol{\kappa})} \}, \mathbf{n}) \left| \hat{W}_{\text{ee}} \right| \overline{\Psi}^{\mathcal{S}_0}(\{ \varphi_{p(\boldsymbol{\kappa})} \}, \mathbf{n}) \right\rangle \\ &\equiv W^{\mathcal{S}_0}(\{ \varphi_{p(\boldsymbol{\kappa})} \}, \mathbf{n}). \end{aligned} \quad (40)$$

For practical purposes, the (less intuitive) expressions in Eqs. (33) and (36) are much more appealing as they do not require the implementation of a specific (seniority-zero in this context) wave function ansatz. Indeed, starting from a regular (seniority-zero) HF calculation, the functional can be evaluated by setting to zero, within the post-HF treatment, the one- and two-electron integrals that do not preserve seniority. The dependence in $\boldsymbol{\kappa}$ of the remaining integrals [see Eq. (29)] enables the optimization of the natural orbitals, as further discussed in the next section.

D. Exact self-consistent seniority-zero equations

Let us start from the regular NOFT [33] variational energy expression that we simply rewrite as follows [see Eqs. (12) and (16)]:

$$E = \min_{\boldsymbol{\kappa}, \mathbf{n}} \left\{ (\mathbf{h}(\boldsymbol{\kappa}) | \mathbf{n}) + W(\boldsymbol{\kappa}, \mathbf{n}) \right\}, \quad (41)$$

where $(\mathbf{h}(\boldsymbol{\kappa}) | \mathbf{n}) = \sum_p h_{pp}(\boldsymbol{\kappa}) n_p$ and

$$h_{pp}(\boldsymbol{\kappa}) = \langle \varphi_p(\boldsymbol{\kappa}) | \hat{h} | \varphi_p(\boldsymbol{\kappa}) \rangle. \quad (42)$$

If we now split the universal interaction functional into seniority-zero and complementary (higher-seniority) parts,

$$\begin{aligned} W(\boldsymbol{\kappa}, \mathbf{n}) &= W^{S_0}(\boldsymbol{\kappa}, \mathbf{n}) + (W(\boldsymbol{\kappa}, \mathbf{n}) - W^{S_0}(\boldsymbol{\kappa}, \mathbf{n})) \\ &= W^{S_0}(\boldsymbol{\kappa}, \mathbf{n}) + \overline{W}^S(\boldsymbol{\kappa}, \mathbf{n}), \end{aligned} \quad (43)$$

the exact ground-state energy can be rewritten [see Eq. (33)] as follows:

$$E = \min_{\boldsymbol{\kappa}, \mathbf{n}} \left\{ \min_{\Psi \rightarrow \mathbf{n}} \left\{ (\mathbf{h}(\boldsymbol{\kappa}) | \mathbf{n}^\Psi) + \langle \Psi | \hat{W}_{ee}^{S_0}(\boldsymbol{\kappa}) | \Psi \rangle + \overline{W}^S(\boldsymbol{\kappa}, \mathbf{n}^\Psi) \right\} \right\}, \quad (44)$$

thus leading to

$$E = \min_{\boldsymbol{\kappa}} \left\{ \min_{\Psi} \left\{ (\mathbf{h}(\boldsymbol{\kappa}) | \mathbf{n}^\Psi) + \langle \Psi | \hat{W}_{ee}^{S_0}(\boldsymbol{\kappa}) | \Psi \rangle + \overline{W}^S(\boldsymbol{\kappa}, \mathbf{n}^\Psi) \right\} \right\}, \quad (45)$$

or, equivalently,

$$E = \min_{\boldsymbol{\kappa}, \Psi} \left\{ \left\langle \sum_p h_{pp}(\boldsymbol{\kappa}) \hat{n}_p + \hat{W}_{ee}^{S_0}(\boldsymbol{\kappa}) \right\rangle_{\Psi} + \overline{W}^S(\boldsymbol{\kappa}, \mathbf{n}^\Psi) \right\} \quad (46)$$

where $\mathbf{n}^\Psi \equiv \{\langle \Psi | \hat{n}_p | \Psi \rangle\}$. We stress again that, unlike in DFT for lattices [116, 118], the energy is obtained in this context by means of a *double* minimization. The first one (with respect to the many-body wave function Ψ) aims at reproducing the natural orbital occupancies. The second one (with respect to $\boldsymbol{\kappa}$), where the one- and two-electron integrals vary [see Eqs. (42) and (29)], respectively],

enables the variational calculation of the natural orbitals.

For convenience, we choose the initial (unrotated) orbital basis to be the exact natural orbital basis of the system under study. In other words, the minimum in Eq. (46) is reached when $\boldsymbol{\kappa} = 0$. By denoting

$$\overline{W}^S(\mathbf{n}) \equiv \overline{W}^S(\boldsymbol{\kappa} = 0, \mathbf{n}), \quad (47)$$

we can reformulate the variational principle as follows:

$$\begin{aligned} E &= \min_{\Psi} \left\{ \langle \Psi | \sum_p h_{pp} \hat{n}_p + \hat{W}_{ee}^{S_0} | \Psi \rangle + \overline{W}^S(\mathbf{n}^\Psi) \right\} \\ &= \sum_p h_{pp} n_p^{\Psi^{S_0}} + \langle \Psi^{S_0} | \hat{W}_{ee}^{S_0} | \Psi^{S_0} \rangle + \overline{W}^S(\mathbf{n}^{\Psi^{S_0}}). \end{aligned} \quad (48)$$

From the corresponding Euler-Lagrange equation, we conclude that the minimizing wave function Ψ^{S_0} , which reproduces the exact natural orbital occupancies, is the ground-state solution to the following self-consistent and seniority-zero Schrödinger-like equation:

$$\hat{\mathcal{H}}^{S_0}(\mathbf{n}^{\Psi^{S_0}}) | \Psi^{S_0} \rangle = \mathcal{E}^{S_0} | \Psi^{S_0} \rangle, \quad (49)$$

where

$$\hat{\mathcal{H}}^{S_0}(\mathbf{n}) = \sum_p \left(h_{pp} + \frac{\partial \overline{W}^S(\mathbf{n})}{\partial n_p} \right) \hat{n}_p + \hat{W}_{ee}^{S_0}. \quad (50)$$

Note that the lower bound in Eq. (48), which is the exact ground-state energy, can be rewritten as follows,

$$E = \left\langle \hat{H} \right\rangle_{\Psi^{S_0}} + \overline{W}^S(\mathbf{n}^{\Psi^{S_0}}), \quad (51)$$

since Ψ^{S_0} is a seniority-zero wave function.

Interestingly, we conclude from Eq. (50) that the diagonal one-electron integral correction introduced in Eq. (11), for the purpose of reproducing the exact natural orbital occupancies, is a density matrix functional quantity which can be evaluated as follows:

$$\bar{\varepsilon}_p = \left. \frac{\partial \overline{W}^S(\mathbf{n})}{\partial n_p} \right|_{\mathbf{n}=\mathbf{n}^{\Psi^{S_0}}}. \quad (52)$$

Further physical insight can be obtained from the seniority separation in Eq. (43), which can be rewritten as follows:

$$\begin{aligned} \overline{W}^S(\mathbf{n}) &= \langle \Psi(\mathbf{n}) | \hat{W}_{ee} | \Psi(\mathbf{n}) \rangle - \langle \Psi^{S_0}(\mathbf{n}) | \hat{W}_{ee}^{S_0} | \Psi^{S_0}(\mathbf{n}) \rangle \\ &= \langle \Psi(\mathbf{n}) | \hat{W}_{ee} | \Psi(\mathbf{n}) \rangle - \langle \Psi^{S_0}(\mathbf{n}) | \hat{W}_{ee} | \Psi^{S_0}(\mathbf{n}) \rangle \\ &= \langle \Psi(\mathbf{n}) | \hat{H} | \Psi(\mathbf{n}) \rangle - \langle \Psi^{S_0}(\mathbf{n}) | \hat{H} | \Psi^{S_0}(\mathbf{n}) \rangle, \end{aligned} \quad (53)$$

where both physical $\Psi(\mathbf{n})$ and seniority-zero $\Psi^{S_0}(\mathbf{n})$ wave functions share, in addition to the occupation numbers \mathbf{n} , the same \mathbf{n} -independent natural orbital basis which, in the present case, is the unrotated orbital basis. As a result, the ‘‘potential’’ $\bar{\varepsilon}_p$ describes the higher-seniority contributions to the energy variation

induced by infinitesimal changes in the natural orbital occupation n_p .

Let us finally emphasize that $\overline{W}^S(\mathbf{n})$ is evaluated with the *exact* natural orbitals. According to Eqs. (45) and (48), the latter can be determined from the following stationarity condition,

$$\left[\begin{aligned} & (\partial \mathbf{h}(\boldsymbol{\kappa}) / \partial \kappa_{pq} | \mathbf{n}^{\Psi^{S_0}}) + \langle \Psi^{S_0} | \partial \hat{W}_{ee}^{S_0}(\boldsymbol{\kappa}) / \partial \kappa_{pq} | \Psi^{S_0} \rangle \\ & + \frac{\partial \overline{W}^S(\boldsymbol{\kappa}, \mathbf{n}^{\Psi^{S_0}})}{\partial \kappa_{pq}} \end{aligned} \right]_{\boldsymbol{\kappa}=0} = 0, \quad (54)$$

which can be rewritten more explicitly as follows [see Appendix B],

$$\begin{aligned} & 2\mathcal{F}_{pq} \left(n_p^{\Psi^{S_0}} - n_q^{\Psi^{S_0}} \right) + \left\langle \varphi_q \left| \frac{\delta \overline{W}^S(\{\varphi_p\}, \mathbf{n}^{\Psi^{S_0}})}{\delta \varphi_p} \right. \right\rangle \\ & - \left\langle \varphi_p \left| \frac{\delta \overline{W}^S(\{\varphi_q\}, \mathbf{n}^{\Psi^{S_0}})}{\delta \varphi_q} \right. \right\rangle \\ & + \sum_r [2\langle rp|rq \rangle - \langle rp|qr \rangle] \\ & \times [(\hat{n}_r - \langle \hat{n}_r \rangle_{\Psi^{S_0}}) \hat{n}_p - (\hat{n}_r - \langle \hat{n}_r \rangle_{\Psi^{S_0}}) \hat{n}_q]_{\Psi^{S_0}} \\ & + 4 \sum_r \langle pq|rr \rangle \\ & \times \left[(1 - \delta_{rp}) \langle \hat{P}_r^\dagger \hat{P}_p \rangle_{\Psi^{S_0}} - (1 - \delta_{rq}) \langle \hat{P}_r^\dagger \hat{P}_q \rangle_{\Psi^{S_0}} \right] = 0, \end{aligned} \quad (55)$$

where $\mathcal{F}_{pq} \equiv \mathcal{F}_{pq}(\{\varphi_r\}, \mathbf{n}^{\Psi^{S_0}})$, and

$$\mathcal{F}_{pq}(\{\varphi_r\}, \mathbf{n}) = h_{pq} + \frac{1}{2} \sum_r [2\langle rp|rq \rangle - \langle rp|qr \rangle] n_r \quad (56)$$

is the density matrix functional Fock matrix element. Note that regular HF and NOFT equations can be recovered from Eq. (55). In both cases, the two summations over the natural orbitals r should be removed, either because they are equal to zero (HF case) or because they are incorporated into the (full) interaction functional $W(\{\varphi_p\}, \mathbf{n})$ [NOFT case]. In the HF case, the complementary (higher-seniority) density matrix functional $\overline{W}^S(\{\varphi_p\}, \mathbf{n})$ is neglected and the usual Fock operator expression for doubly occupied orbitals is recovered:

$$\mathcal{F}_{pq} \xrightarrow{\text{HF}} h_{pq} + \sum_r^{\text{occ.}} [2\langle rp|rq \rangle - \langle rp|qr \rangle], \quad (57)$$

thus leading to the HF equations. In the NOFT case, one would proceed with the following substitutions,

$$\begin{aligned} & \mathcal{F}_{pq} \xrightarrow{\text{NOFT}} h_{pq}, \\ & \overline{W}^S(\{\varphi_p\}, \mathbf{n}) \xrightarrow{\text{NOFT}} W(\{\varphi_p\}, \mathbf{n}), \end{aligned} \quad (58)$$

thus leading to the regular NOFT equations for the natural orbitals [33]. In the latter case, the occupation numbers are directly used as basic variables, *i.e.* they are not calculated from an auxiliary many-body wave function, unlike in the present approach. The construction of density matrix functional approximations to $\overline{W}^S(\{\varphi_p\}, \mathbf{n})$ as well as the self-consistent implementation of Eq. (55), which are essential for turning the theory into a practical computational method, are left for future work. In the rest of this work, we assume that the exact natural orbitals of the system under study are known and we focus on the evaluation of the complementary (higher-seniority) natural orbital occupation functional energy $\overline{W}^S(\mathbf{n}^{\Psi^{S_0}})$ [see Eq. (48)].

III. ADIABATIC CONNECTION FORMALISMS

We focus in the following on the practical evaluation of the complementary higher-seniority correlation energy $\overline{W}^S(\mathbf{n}^{\Psi^{S_0}})$ [see Eq. (51)] which has been described in the previous sections as an implicit functional of the density matrix. For that purpose, we derive in Sec. III A an exact adiabatic connection (AC) formula in the basis of the exact natural orbitals. Along such a (so-called constrained) AC path, the occupation of the (true) natural orbitals is held constant. Approximations along the AC (based either on second-order perturbation theory or linear interpolations) are then discussed in Sec. III B. For analysis purposes, we finally investigate in Sec. III C a simpler AC where the natural orbital occupations constraint is relaxed. In this case, the reference seniority-zero wave function does not reproduce the true density matrix anymore. Nevertheless, integrating over the full relaxed AC path will still provide the exact ground-state energy. For comparison with the constrained AC, we also derive a second-order perturbation theory along the relaxed AC. The performance of the various approximations will be discussed in the separate Sec. V.

A. Exact constrained adiabatic connection

In order to obtain further insight into the higher-seniority natural orbital occupation functional of Eq. (47), we propose to construct an AC path between the fictitious seniority-zero Ψ^{S_0} wave function and the physical (fully-interacting) one Ψ_0 in the *exact natural orbital basis of the latter* $\{\varphi_p\}$. For that purpose, we consider the following partially-interacting (ground-state) Schrödinger equation,

$$\hat{H}^\lambda |\Psi_0^\lambda\rangle = \mathcal{E}_0^\lambda |\Psi_0^\lambda\rangle, \quad (59)$$

where λ varies continuously in the range $0 \leq \lambda \leq 1$. Note that we label as “0” the ground state along the AC since the excited states will come into play (later in

Sec. III B) when solving \hat{H}^λ in perturbation theory.

Let us denote

$$\hat{H}^\lambda \equiv \hat{H}^\lambda(\boldsymbol{\varepsilon}^\lambda) \quad (60)$$

and $\mathcal{E}_0^\lambda \equiv \mathcal{E}_0^\lambda(\boldsymbol{\varepsilon}^\lambda)$, where the partially-interacting Hamiltonian reads as follows, for an arbitrary potential $\boldsymbol{\varepsilon} \equiv \{\varepsilon_p\}$,

$$\hat{H}^\lambda(\boldsymbol{\varepsilon}) = \sum_p \varepsilon_p \hat{n}_p + \hat{W}_{ee}^{S_0} + \lambda \hat{V}, \quad (61)$$

$$\hat{V} = \hat{W}_{ee} - \hat{W}_{ee}^{S_0} + \sum_{p \neq q} h_{pq} \hat{n}_{pq}, \quad (62)$$

and $\hat{n}_{pq} = \sum_\sigma \hat{a}_{p\sigma}^\dagger \hat{a}_{q\sigma}$. The potential $\boldsymbol{\varepsilon}^\lambda \equiv \{\varepsilon_p^\lambda\}$ is determined along the AC from the natural orbital occupation constraint

$$\left\{ \langle \hat{n}_p \rangle_{\Psi_0^\lambda} \right\} \equiv \mathbf{n}^{\Psi_0^\lambda} = \mathbf{n}^{\Psi_0} = \mathbf{n}^{\Psi^{S_0}}, \quad (63)$$

which, in complete analogy with Eq. (36), can be rewritten as a Lieb maximization problem [119]:

$$\boldsymbol{\varepsilon}^\lambda = \arg \max_{\boldsymbol{\varepsilon}} \left\{ \mathcal{E}_0^\lambda(\boldsymbol{\varepsilon}) - (\boldsymbol{\varepsilon} | \mathbf{n}^{\Psi_0}) \right\}, \quad (64)$$

where $\mathcal{E}_0^\lambda(\boldsymbol{\varepsilon})$ is the ground-state energy of $\hat{H}^\lambda(\boldsymbol{\varepsilon})$.

As readily seen from Eq. (61), for $\lambda = 1$, the true physical Hamiltonian is recovered when $\varepsilon_p^{\lambda=1} = h_{pp}$ (the orbital occupation constraint of Eq. (63) is fulfilled in this case), thus leading to

$$\mathcal{E}_0^{\lambda=1} = E = (\boldsymbol{\varepsilon}^{\lambda=1} | \mathbf{n}^{\Psi_0}) + \langle \hat{W}_{ee} \rangle_{\Psi_0}, \quad (65)$$

where we used the fact that, by construction,

$$\langle \hat{n}_{pq} \rangle_{\Psi_0} \stackrel{p \neq q}{=} 0. \quad (66)$$

On the other hand, the seniority-zero wave function Ψ^{S_0} with the same occupation numbers is recovered when $\lambda = 0$, thus leading to the following simplified energy expression,

$$\mathcal{E}_0^{\lambda=0} = \langle \hat{W}_{ee}^{S_0} \rangle_{\Psi^{S_0}} + (\boldsymbol{\varepsilon}^{\lambda=0} | \mathbf{n}^{\Psi_0}). \quad (67)$$

We stress that, by construction, the density matrix (which is here evaluated in the exact physical natural orbital basis) is diagonal in both $\lambda = 0$ and $\lambda = 1$ limits. However, unlike in Ref. 48, we do *not* assume or expect the density matrix to remain strictly diagonal along the AC. The present AC relies on an orbital occupation constraint, not on a density matrix one. Nevertheless, for the systems discussed in Sec. V, we have observed numerically that the off-diagonal elements of the 1RDM do not deviate substantially from zero when $0 < \lambda < 1$.

We can now evaluate along the AC path the complementary higher-seniority correlation energy of Eq. (53),

in the particular case where $\mathbf{n} = \mathbf{n}^{\Psi_0} = \mathbf{n}^{\Psi^{S_0}}$. From the original expression

$$\overline{W}^S \equiv \overline{W}^S(\mathbf{n}^{\Psi_0}) = \langle \hat{W}_{ee} \rangle_{\Psi_0} - \langle \hat{W}_{ee}^{S_0} \rangle_{\Psi^{S_0}}, \quad (68)$$

which can be rewritten as follows [see Eq. (65) and Eq. (67)],

$$\overline{W}^S = [\mathcal{E}_0^\lambda - (\boldsymbol{\varepsilon}^\lambda | \mathbf{n}^{\Psi_0})]_{\lambda=1} - [\mathcal{E}_0^\lambda - (\boldsymbol{\varepsilon}^\lambda | \mathbf{n}^{\Psi_0})]_{\lambda=0}, \quad (69)$$

we obtain the following exact AC formula,

$$\overline{W}^S = \int_0^1 d\lambda \left[\frac{\partial \mathcal{E}_0^\lambda}{\partial \lambda} - \left(\frac{\partial \boldsymbol{\varepsilon}^\lambda}{\partial \lambda} | \mathbf{n}^{\Psi_0} \right) \right] \quad (70)$$

$$= \int_0^1 d\lambda \overline{W}^{S,\lambda}, \quad (71)$$

where, according to the Hellmann–Feynman theorem and the orbital occupation constraint of Eq. (63), the higher-seniority integrand reads

$$\overline{W}^{S,\lambda} = \langle \hat{V} \rangle_{\Psi_0^\lambda} \quad (72)$$

$$= \langle \hat{W}_{ee} - \hat{W}_{ee}^{S_0} \rangle_{\Psi_0^\lambda} + \sum_{p \neq q} h_{pq} \langle \hat{n}_{pq} \rangle_{\Psi_0^\lambda}. \quad (73)$$

Note that $\overline{W}^{S,\lambda=0} = 0$, by construction. Moreover, as pointed out previously, $\langle \hat{n}_{pq} \rangle_{\Psi_0^\lambda}$ vanishes in both fully-interacting ($\lambda = 1$) and seniority-zero ($\lambda = 0$) limits but it can in principle deviate from zero when $0 < \lambda < 1$.

Once the λ -dependent integrand is determined, the total ground-state energy can be evaluated, in principle exactly, as follows [see Eq. (51)],

$$E = \langle \hat{H} \rangle_{\Psi^{S_0}} + \int_0^1 d\lambda \overline{W}^{S,\lambda}. \quad (74)$$

The above formula and Eq. (73) are interesting in several ways. Firstly, as readily seen, the integrand plays a central role in the description of higher-seniority energy contributions. Secondly, they can serve as a basis for the development of approximations, as discussed further in the following.

B. Approximations along the adiabatic connection

As done before in the context of DFT [see, for example, Refs. [120, 121] and the references therein], we can construct various approximate schemes by simplifying the integrand expression. For example, by analogy with Görling–Levy second-order perturbation theory (PT2) [122, 123], we may assume that the integrand

varies linearly (with the slope obtained in the seniority-zero $\lambda = 0$ limit) along the AC:

$$\overline{\mathcal{W}}^{S,\lambda} \stackrel{\text{PT2}}{\approx} \lambda \left. \frac{\partial \overline{\mathcal{W}}^{S,\lambda}}{\partial \lambda} \right|_{\lambda=0}. \quad (75)$$

According to Eq. (72) and perturbation theory that we apply to Eq. (59) with an infinitesimal variation of the higher-seniority strength parameter λ , the first-order derivative of the integrand can be expressed analytically as follows,

$$\frac{\partial \overline{\mathcal{W}}^{S,\lambda}}{\partial \lambda} = 2 \left\langle \Psi_0^\lambda \left| \hat{\mathcal{V}} \left| \frac{\partial \Psi_0^\lambda}{\partial \lambda} \right. \right. \right\rangle \quad (76)$$

$$= 2 \sum_{I>0} \frac{\langle \Psi_0^\lambda | \hat{\mathcal{V}} | \Psi_I^\lambda \rangle \langle \Psi_I^\lambda | \frac{\partial \hat{H}^\lambda}{\partial \lambda} | \Psi_0^\lambda \rangle}{\mathcal{E}_0^\lambda - \mathcal{E}_I^\lambda}, \quad (77)$$

or, more explicitly [see Eqs. (60) and (61)],

$$\begin{aligned} \frac{\partial \overline{\mathcal{W}}^{S,\lambda}}{\partial \lambda} &= 2 \sum_{I>0} \frac{\langle \Psi_0^\lambda | \hat{\mathcal{V}} | \Psi_I^\lambda \rangle}{\mathcal{E}_0^\lambda - \mathcal{E}_I^\lambda} \\ &\quad \times \langle \Psi_I^\lambda | \hat{\mathcal{V}} + \sum_p \frac{\partial \varepsilon_p^\lambda}{\partial \lambda} \hat{n}_p | \Psi_0^\lambda \rangle, \end{aligned} \quad (78)$$

where the summation runs over the excited states of \hat{H}^λ . Note that, in the $\lambda = 0$ limit, the excited states that contribute to the perturbation expansion should be coupled to the seniority-zero ground-state wave function Ψ^{S_0} through the higher-seniority Hamiltonian term $\hat{\mathcal{V}}$:

$$\langle \Psi^{S_0} | \hat{\mathcal{V}} | \Psi_I^{\lambda=0} \rangle \neq 0. \quad (79)$$

Obviously, pure seniority-zero solutions will be automatically excluded from the expansion. In other words, only pure higher-seniority solutions [124–126] to $\hat{H}^{\lambda=0}$ will contribute. Note also that, in complete analogy with Görling–Levy PT [122, 123], the integrand derivative can be rewritten as a PT2 energy correction. Indeed, according to the natural orbital occupations constraint of Eq. (63),

$$0 = \frac{\partial \langle \hat{n}_p \rangle_{\Psi_0^\lambda}}{\partial \lambda} = 2 \left\langle \Psi_0^\lambda \left| \hat{n}_p \left| \frac{\partial \Psi_0^\lambda}{\partial \lambda} \right. \right. \right\rangle, \quad (80)$$

thus leading to

$$\begin{aligned} \left\langle \Psi_0^\lambda \left| \hat{\mathcal{V}} \left| \frac{\partial \Psi_0^\lambda}{\partial \lambda} \right. \right. \right\rangle &= \left\langle \Psi_0^\lambda \left| \hat{\mathcal{V}} + \sum_p \frac{\partial \varepsilon_p^\lambda}{\partial \lambda} \hat{n}_p \left| \frac{\partial \Psi_0^\lambda}{\partial \lambda} \right. \right. \right\rangle \\ &= \left\langle \Psi_0^\lambda \left| \frac{\partial \hat{H}^\lambda}{\partial \lambda} \left| \frac{\partial \Psi_0^\lambda}{\partial \lambda} \right. \right. \right\rangle, \end{aligned} \quad (81)$$

and, consequently [see Eq. (76)],

$$\frac{\partial \overline{\mathcal{W}}^{S,\lambda}}{\partial \lambda} = 2 \left\langle \Psi_0^\lambda \left| \frac{\partial \hat{H}^\lambda}{\partial \lambda} \left| \frac{\partial \Psi_0^\lambda}{\partial \lambda} \right. \right. \right\rangle. \quad (82)$$

Finally, from the first-order perturbation expansion in λ of Ψ_0^λ [see Eq. (77)], we do recover (with a factor 2) a second-order energy correction:

$$\begin{aligned} \frac{\partial \overline{\mathcal{W}}^{S,\lambda}}{\partial \lambda} &= 2 \sum_{I>0} \frac{\left| \langle \Psi_0^\lambda | \frac{\partial \hat{H}^\lambda}{\partial \lambda} | \Psi_I^\lambda \rangle \right|^2}{\mathcal{E}_0^\lambda - \mathcal{E}_I^\lambda} \\ &= 2 \sum_{I>0} \frac{\left| \langle \Psi_0^\lambda | \hat{\mathcal{V}} + \sum_p \frac{\partial \varepsilon_p^\lambda}{\partial \lambda} \hat{n}_p | \Psi_I^\lambda \rangle \right|^2}{\mathcal{E}_0^\lambda - \mathcal{E}_I^\lambda}. \end{aligned} \quad (83)$$

If we return to Eq. (75), integrating over the range $0 \leq \lambda \leq 1$ [see Eq. (74)] leads to the following PT2-like total energy expression,

$$E \stackrel{\text{PT2}}{\approx} \langle \hat{H} \rangle_{\Psi^{S_0}} + \frac{1}{2} \left. \frac{\partial \overline{\mathcal{W}}^{S,\lambda}}{\partial \lambda} \right|_{\lambda=0}. \quad (84)$$

As an alternative to PT2 for evaluating higher-seniority correlation energies we may use linear interpolations (LIs) of the AC integrand. In the simplest LI, we interpolate between the seniority-zero ($\lambda = 0$) and fully-interacting ($\lambda = 1$) limits. We refer to this approximation as *one-segment* LI (1LI):

$$\overline{\mathcal{W}}^{S,\lambda} \stackrel{\text{1LI}}{\approx} \lambda \overline{\mathcal{W}}^{S,\lambda=1}, \quad (85)$$

which gives the following energy expression after integration over λ ,

$$E \stackrel{\text{1LI}}{\approx} \langle \hat{H} \rangle_{\Psi^{S_0}} + \frac{1}{2} \overline{\mathcal{W}}^{S,\lambda=1}. \quad (86)$$

We also consider in the present work a refined *two-segment* LI (2LI) where we first linearly interpolate the integrand in the range $0 \leq \lambda \leq 1/2$ and then in $1/2 \leq \lambda \leq 1$, *i.e.*,

$$\begin{aligned} \overline{\mathcal{W}}^{S,\lambda} \stackrel{\text{2LI}}{\approx} &2\lambda \overline{\mathcal{W}}^{S,\lambda=1/2} \mathcal{I}_{[0,1/2]}(\lambda) \\ &+ \left[2\lambda \left(\overline{\mathcal{W}}^{S,\lambda=1} - \overline{\mathcal{W}}^{S,\lambda=1/2} \right) \right. \\ &\left. + 2\overline{\mathcal{W}}^{S,\lambda=1/2} - \overline{\mathcal{W}}^{S,\lambda=1} \right] \times \mathcal{I}_{[1/2,1]}(\lambda), \end{aligned} \quad (87)$$

where the indicator function is defined as follows,

$$\mathcal{I}_A(\lambda) = \begin{cases} 1 & \lambda \in A \\ 0 & \lambda \notin A \end{cases}. \quad (88)$$

The corresponding 2LI energy, which is obtained by integrating over $0 \leq \lambda \leq 1$, reads

$$E \stackrel{\text{2LI}}{\approx} \langle \hat{H} \rangle_{\Psi^{S_0}} + \frac{1}{2} \overline{\mathcal{W}}^{S,\lambda=1/2} + \frac{1}{4} \overline{\mathcal{W}}^{S,\lambda=1}. \quad (89)$$

The performance of the various approximations we have introduced within the present constrained AC (*i.e.*, 1LI, 2LI, and PT2) will be discussed in detail in Sec. V.

C. Relaxed adiabatic connection

For analysis purposes, we consider another (simpler) AC formalism where the λ -independent physical potential $\varepsilon_p^{\lambda=1} = h_{pp}$ is employed along the AC path, thus relaxing the natural orbital occupations constraint of Eq. (63). In this *relaxed* AC, the partially-interacting Schrödinger equation reads

$$\left(\sum_p h_{pp} \hat{n}_p + \hat{W}_{ee}^{S_0} + \lambda \hat{V} \right) \left| \tilde{\Psi}_0^\lambda \right\rangle = \tilde{\varepsilon}_0^\lambda \left| \tilde{\Psi}_0^\lambda \right\rangle. \quad (90)$$

The $\lambda = 0$ case corresponds to a DOCI-like calculation, where a straight minimization of the energy $\langle \hat{H} \rangle$ is performed over seniority-zero wave functions (constructed here from the exact natural orbitals):

$$\tilde{\varepsilon}_0^{\lambda=0} = \min_{\Psi \in S_0} \langle \hat{H} \rangle_\Psi = \langle \hat{H} \rangle_{\tilde{\Psi}^{S_0}}. \quad (91)$$

Unlike the reference seniority-zero wave function Ψ^{S_0} introduced previously, which is a functional of the ground-state density matrix, the minimizing $\tilde{\Psi}^{S_0} = \tilde{\Psi}_0^{\lambda=0}$ solution does *not* necessarily reproduce the exact natural orbital occupancies. Since the true (physical) Schrödinger equation is recovered from Eq. (90) when $\lambda = 1$, the *exact* ground-state energy can be expressed as follows,

$$E = \tilde{\varepsilon}_0^{\lambda=1} = \tilde{\varepsilon}_0^{\lambda=0} + \int_0^1 d\lambda \frac{\partial \tilde{\varepsilon}_0^\lambda}{\partial \lambda}, \quad (92)$$

or, equivalently [see Eq. (91)],

$$E = \langle \hat{H} \rangle_{\tilde{\Psi}^{S_0}} + \int_0^1 d\lambda \tilde{W}^{S,\lambda}, \quad (93)$$

where, according to the Hellmann–Feynman theorem and Eq. (90), the relaxed AC integrand reads

$$\tilde{W}^{S,\lambda} = \frac{\partial \tilde{\varepsilon}_0^\lambda}{\partial \lambda} = \langle \hat{V} \rangle_{\tilde{\Psi}_0^\lambda}. \quad (94)$$

By analogy with Eqs. (75) and (84), an approximate PT2 scheme can be derived along the relaxed AC if we assume that the integrand varies linearly in λ , *i.e.*,

$$\tilde{W}^{S,\lambda} \underset{\text{relaxed AC}}{\overset{\text{PT2}}{\approx}} \lambda \left. \frac{\partial \tilde{W}^{S,\lambda}}{\partial \lambda} \right|_{\lambda=0}, \quad (95)$$

thus leading to the following PT2-like energy expression after integration over λ :

$$E \underset{\text{relaxed AC}}{\overset{\text{PT2}}{\approx}} \langle \hat{H} \rangle_{\tilde{\Psi}^{S_0}} + \frac{1}{2} \left. \frac{\partial \tilde{W}^{S,\lambda}}{\partial \lambda} \right|_{\lambda=0}. \quad (96)$$

According to perturbation theory that we apply to the relaxed AC Hamiltonian of Eq. (90) with an infinitesimal

variation of λ , the first-order derivative of the relaxed AC integrand reads more explicitly

$$\frac{\partial \tilde{W}^{S,\lambda}}{\partial \lambda} = 2 \sum_{I>0} \frac{\langle \tilde{\Psi}_0^\lambda | \hat{V} | \tilde{\Psi}_I^\lambda \rangle \langle \tilde{\Psi}_I^\lambda | \hat{V} | \tilde{\Psi}_0^\lambda \rangle}{\tilde{\varepsilon}_0^\lambda - \tilde{\varepsilon}_I^\lambda}. \quad (97)$$

Note that, unlike the 1LI or 2LI approximations that have been introduced in Sec. III B, PT2 relies solely on pure zero- and higher-seniority wave functions. As further discussed in Sec. V, in relatively weak correlation regimes, PT2 systematically overestimates the higher-seniority correlation energy, when applied to the constrained AC. Its performance dramatically improves when the relaxed AC path is followed instead.

IV. COMPUTATIONAL DETAILS

The reverse engineering procedure described in Eq. (64), where the true natural orbital occupancies $\{n_p^{\Psi_0}\}$ are used as input in the Lieb maximization, has been implemented together with the Block *density matrix renormalization group* (DMRG) code [127–132]. The DMRG code is used to obtain the ground-state energy of the λ -dependent Hamiltonian [see Eqs. (59) and (61)] for any λ in $0 \leq \lambda \leq 1$. The natural orbitals were obtained by diagonalizing the 1RDM from the reference calculation (FCI or DMRG) in the canonical orbital basis. The DIIS algorithm has been used to find a set of potential values $\{\varepsilon_p^\lambda\}$ which satisfies

$$n_p^{\Psi_0^\lambda(\{\varepsilon_p^\lambda\})} - n_p^{\Psi_0} \stackrel{!}{=} 0. \quad (98)$$

The threshold for convergence of the DMRG sweep energies has been set to 10^{-10} Hartree, and threshold for the Euclidian norm of the residual in Eq. (98) has been set to 10^{-5} . As a proof of concept, we test our method on the metallic H_4 linear chain (considering symmetric stretching) in the STO-3G basis, the metallic H_8 linear chain in the cc-pVDZ basis, and the Helium dimer [133] in the cc-pVDZ basis. In the latter case, no basis set superposition error (BSSE) corrections have been applied so that a direct comparison can be made with the results of Ref. [96]. The number of renormalized states in the DMRG calculation is set to $m = 400$ for He_2 , and $m = 800$ for H_8 . In the latter case, the DMRG energy with respect to m converged with an order of 10^{-5} Hartree (see Appendix D). Molcas [134] has been used to compute the one- and two-body electronic integrals. In order to further analyze the AC integrand in the case of the H_4 chain in the minimal basis (in particular its variation along the AC), Psi4 [135] was used to generate the electronic integrals and OpenFermion [136] was used to construct the (λ -dependent) Hamiltonian that is then diagonalized exactly in the subspace conserving the number of particles and spin singlet.

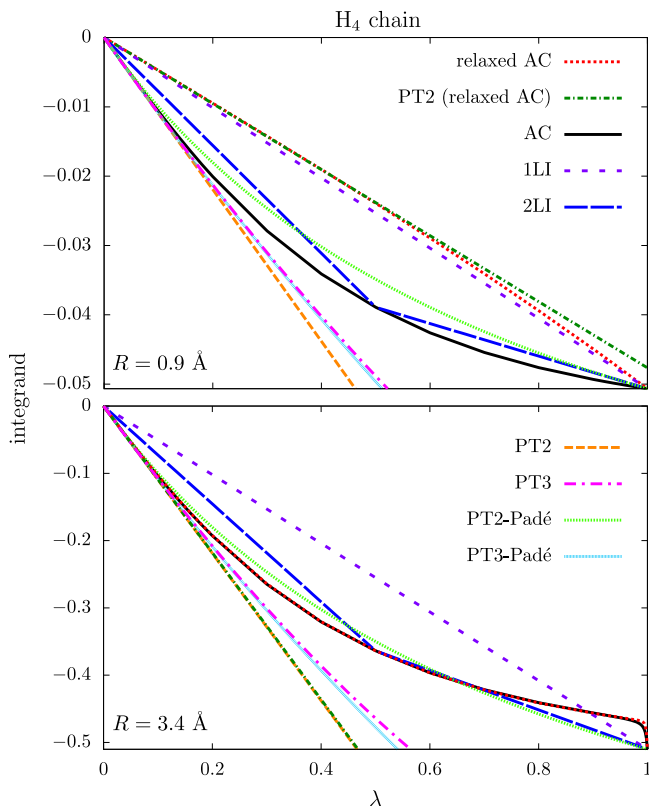


FIG. 1. “Exact” and approximate higher-seniority correlation integrands evaluated along the constrained (simply referred to as AC) and relaxed ACs for the H_4 chain with interatomic distances $R = 0.9 \text{ \AA}$ (top panel) and $R = 3.4 \text{ \AA}$ (bottom panel). Energies are in atomic unit (hartree). See text for further details.

V. RESULTS AND DISCUSSION

A. H_4 chain in a minimal basis

1. AC and potential energy curves

Let us start with the H_4 linear chain in the minimal basis STO-3G. The “exact” (*i.e.*, exact in the considered minimal basis) and approximate integrands are shown in Fig. 1 for interatomic distances $R = 0.9 \text{ \AA}$ (top panel) and $R = 3.4 \text{ \AA}$ (bottom panel) corresponding to a weakly and strongly correlated regimes, respectively. In analogy with the one obtained in the approach of Pernal [49], our exact AC integrand has a quadratic behaviour with respect to λ . However, it shows a much more pronounced curvature so that the 1LI approximation, the PT2 approximation, or the linear extrapolation schemes proposed in Ref. [48], are expected to be less accurate. To improve over the PT2 approximation, the PT3 approximation as well as Padé approximants have been considered for the constrained AC, and are detailed in Appendix C. As readily seen in Fig. 1, while the PT3 and PT3-Padé approximations show some curvature,

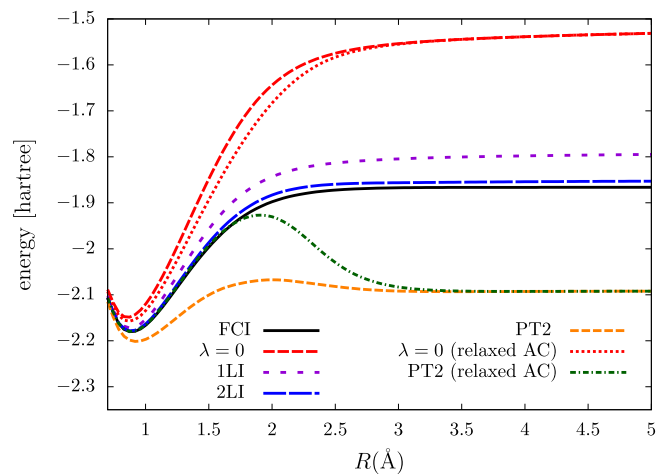


FIG. 2. Potential energy curves plotted for the H_4 chain (with equidistant hydrogen atoms) at both seniority-zero ($\lambda = 0$), which is equivalent to perturbation theory through first order, and higher-seniority (1LI, 2LI, or PT2) levels of approximation within the constrained AC. Results obtained from the relaxed AC are shown for analysis purposes. See text for further details.

they are still not sufficiently accurate. In contrast, the PT2-Padé approximant – which is exact in the $\lambda \rightarrow 0$ and $\lambda \rightarrow 1$ limits of the AC integrand – recovers a large part of the curvature by construction.

We show in Fig. 2 the potential energy curves generated from both the AC with the natural orbital occupation constraint (that we simply refer to as constrained AC in the following) and its relaxed version, with and without higher-seniority correlation energy corrections [see Eqs. (84), (86), (89), and (96)]. Equilibrium bond distances and total energies as well as dissociation energies are also provided in Table I. We see that the relaxed and constrained seniority-zero ($\lambda = 0$) wave functions slightly underestimate the bond distance (in comparison with FCI). However, they both overestimate (by about 100%) the dissociation energy. The PT2 approximation to the constrained AC systematically overestimates (roughly by 100% for all bond distances) the higher-seniority correlation energy, with a large error on the total energy when the chain is stretched. As shown in Table I, at this level of approximation, the equilibrium bond distance is too long (in comparison with FCI) and the dissociation energy is dramatically underestimated. On the other hand, approximating the constrained AC integrand with a linear interpolation over the entire interaction strength $0 \leq \lambda \leq 1$ (1LI approximation) gives much better (although too high) total energies. The equilibrium bond distance is relatively accurate in this case (see Table I). The error increases along the dissociation coordinate R but remains substantially smaller than that of PT2. The 1LI approximation substantially improves the description of the dissociation energy. Linearly interpolating over

the two segments $0 \leq \lambda \leq 1/2$ and $1/2 \leq \lambda \leq 1$ (2LI approximation) is, by construction, designed to better account for the quadratic behaviour of the constrained AC integrand (see Fig. 1), thus providing more accurate total energies for all bond distances, as expected.

Let us now focus on the relaxed AC results. Unlike in the constrained AC, the DOCI coefficients of the reference seniority-zero wave function are determined by energy minimization. They are not expected to reproduce the “exact” natural orbital occupancies but will obviously give a lower (although not substantially better, even at equilibrium) total energy when the higher-seniority correlation energy is neglected (see the “ $\lambda = 0$ ” curves in Fig. 2). More interestingly, around equilibrium, the relaxed AC integrand exhibits a very weak curvature (see the top panel of Fig. 1) Therefore, the PT2 approximation to the relaxed AC (see Fig. 2) gives very accurate total energies for bond distances shorter than $R = 1.75 \text{ \AA}$. Beyond this distance the results dramatically deteriorate and, for $R > 3.4 \text{ \AA}$, the relaxed and constrained ACs give the same total energies at the PT2 level of approximation. As a result, the PT2 description of the dissociation energy worsens even further when relaxing the AC (see Table I). As shown in Fig. 2, in the latter case, the seniority-zero total energy is the same (whether the AC is relaxed or not). Moreover, for $R = 3.4 \text{ \AA}$, the two AC integrands are indistinguishable not only around $\lambda = 0$, as expected from the PT2 results, but also for larger higher-seniority interaction strength values λ (see the bottom panel of Fig. 1). Slight differences only appear in the vicinity of $\lambda = 1$.

2. Potential and integrand slope along the AC

For further comparison of the constrained and relaxed ACs at equilibrium and stretched geometries, we show in Fig. 3 “exact” potential values ε_p^λ over the natural orbital space ($1 \leq p \leq 4$) and along the constrained AC (*i.e.*, for $0 \leq \lambda \leq 1$). As readily seen from the top panel of Fig. 3, variations in λ are quite substantial when $R = 0.9 \text{ \AA}$. We recall that the λ -independent potential $\{\varepsilon_p^{\lambda=1}\}$ is employed in the relaxed AC, thus suggesting that constrained and relaxed AC curves should indeed be different at equilibrium (the impact of the potential on the shape of the AC integrand will be further rationalized in the following). In contrast, in the stretched $R = 3.4 \text{ \AA}$ geometry, the dependence in λ of the potential is drastically reduced (see the bottom panel of Fig. 3). Indeed, in this case, the deviation $|\varepsilon_p^\lambda - \varepsilon_p^{\lambda=1}|$ from the fully-interacting ($\lambda = 1$) potential never exceeds 7 millihartrees, against 0.5 hartrees at equilibrium (see the top panel of Fig. 3). This explains why the constrained and relaxed AC curves are essentially on top of each other when $R = 3.4 \text{ \AA}$ (see the bottom panel of Fig. 1). At this point we should emphasize that the natural orbitals become singly occupied in the dissociation limit. As a

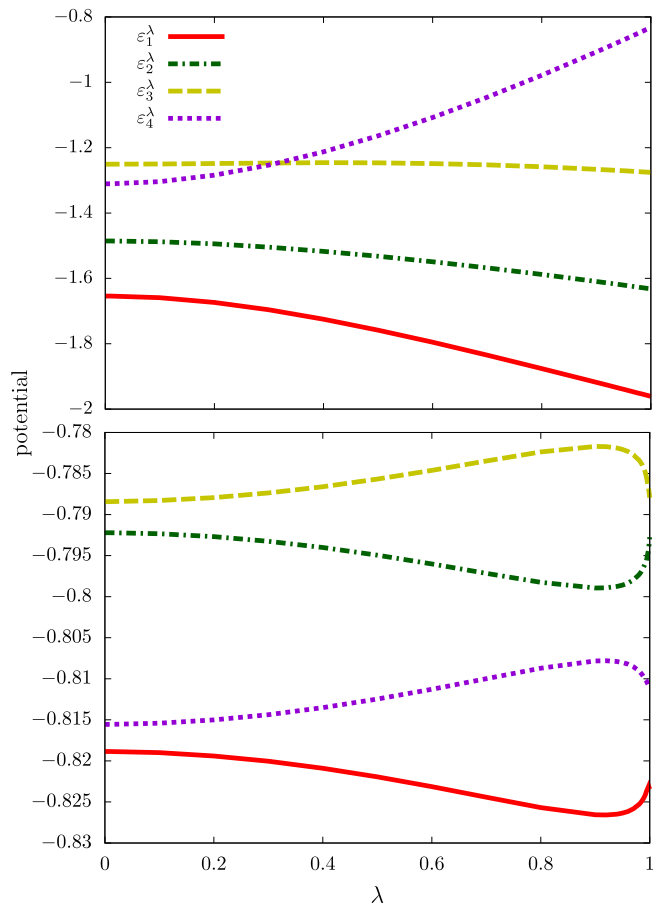


FIG. 3. Potential values $\{\varepsilon_p^\lambda\}$ computed along the constrained AC [see Eq. (64)] for the H_4 molecular chain in a minimal basis with interatomic distances $R = 0.9 \text{ \AA}$ (top panel) and $R = 3.4 \text{ \AA}$ (bottom panel). Energies are in atomic unit (hartree).

result, in the present minimal basis, the density matrix becomes the identity matrix and the natural orbitals can be arbitrarily rotated. In the stretched $R = 3.4 \text{ \AA}$ geometry, the natural orbital occupations are closed (but not strictly equal) to 1. Even though the natural orbitals are slightly more localized, their expansion over the atomic orbitals resembles that of the canonical HF orbitals in this case.

In order to further rationalize the shape of the constrained and relaxed AC integrands, it is actually instructive to look at their slopes in λ along the AC. Exact analytical expressions are trivially obtained from static perturbation theory [see Eqs. (83) and (97), respectively]. At equilibrium, the substantial variations in λ of the potential along the constrained AC are expected to be reflected in the excitation energies $\mathcal{E}_I^\lambda - \mathcal{E}_0^\lambda$ (*i.e.*, the denominators in the perturbation expansion). We do observe this feature numerically, as shown in the top panels of Figs. 4 and 5 for the first and fourth excited state, respectively. Unlike the former, the latter couples to the ground state along the AC and the resulting contribution to the perturbation expansion is significant. Note that, as readily

| H ₄ | R_{eq} (Å) | Equilibrium energy | Dissociation energy |
|----------------------------|---------------------|--------------------|---------------------|
| $\lambda = 0$ | 0.86 | -2.148979 | 0.617577 |
| $\lambda = 0$ (relaxed AC) | 0.87 | -2.157561 | 0.626158 |
| PT2 | 0.94 | -2.201520 | 0.109404 |
| PT2 (relaxed AC) | 0.89 | -2.179969 | 0.087854 |
| 1LI | 0.88 | -2.172768 | 0.378017 |
| 2LI | 0.89 | -2.178426 | 0.325506 |
| $\lambda = 1$ (FCI) | 0.89 | -2.180501 | 0.314174 |

TABLE I. Equilibrium bond distance, total energy at equilibrium, and dissociation energy (in Hartree) of the H₄ chain computed in the minimal STO-3G basis at the constrained and relaxed seniority-zero ($\lambda = 0$) levels of approximation (which is equivalent to perturbation theory through first order) and beyond. In the latter case, PT2, 1LI or 2LI energy corrections are applied [see Eqs. (84), (86) and (89) for the constrained AC, and Eq. (96) for the relaxed AC]. Comparison is made with FCI. The dissociation energy is simply evaluated as the difference between the energies at $R = 5$ Å and $R = R_{\text{eq}}$. See text for further details.

seen in Eqs. (83) and (97), AC integrand slopes will always be negative, like a second-order ground-state energy correction in perturbation theory. In the relaxed AC, the fourth excitation energy is much smaller than that of the constrained AC away from the fully-interacting $\lambda = 1$ limit, especially in the vicinity of the seniority-zero ($\lambda = 0$) limit. This is the reason why the constrained AC integrand has a much steeper slope at $\lambda = 0$ (see the top panel of Fig. 1). Finally, the expected quasi-independence in λ of the excitation energies along the relaxed AC, which leads to a relatively weak dependence in λ of the integrand slope (especially for $\lambda \leq 0.5$), explains why the PT2 approximation is relatively accurate in this case (see the top panel of Fig. 1). Turning to the stretched $R = 3.4$ Å geometry, the above mentioned weak dependence in λ of the potential along the constrained AC explains why the relaxed AC essentially gives the same excitation energies (see the bottom panels of Figs. 4 and 5) and, ultimately, to the same AC curves. The slight differences observed in the vicinity of the fully-interacting $\lambda = 1$ limit (see the bottom panel of Fig. 1) can be traced back to the coupling (through higher-seniority contributions to the Hamiltonian) between the ground and first excited states, as shown in the bottom panel of Fig. 4. We can also relate the sudden drop in slope, which is a peculiar feature that both constrained and relaxed ACs exhibit when approaching the latter limit, to both the increase of the coupling and the drop of the first excitation energy. This feature appears when the bond distance is larger than $R = 2$ Å (not shown). As shown in Fig. 2, this is precisely the distance at which the PT2 description of the constrained AC is not accurate anymore.

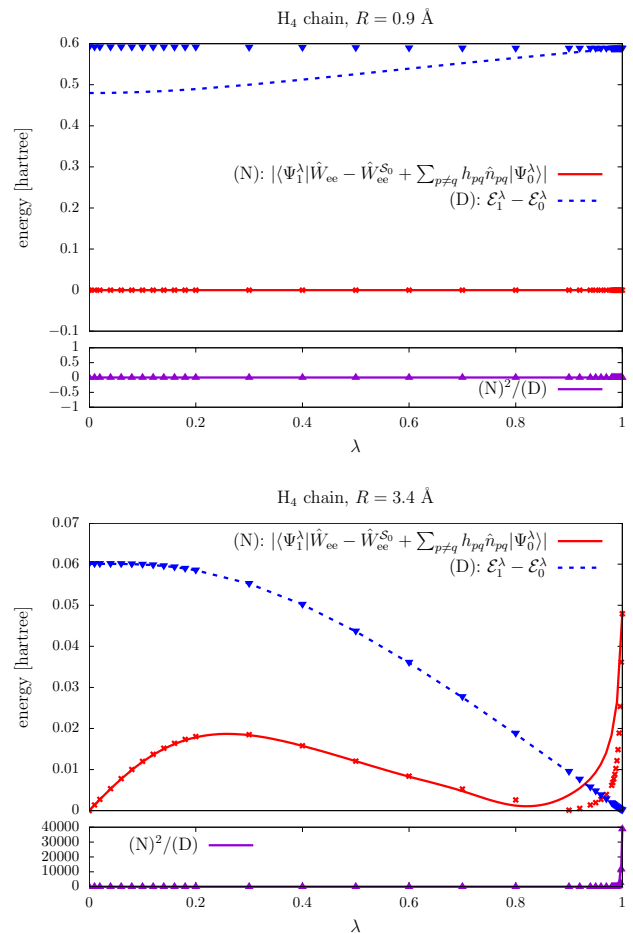


FIG. 4. Detailed first-excited-state contribution to the derivative in λ of the constrained (solid and dashed lines) and relaxed (solid dots) AC integrands [see Eqs. (83) and (97)]. The two upper and lower panels correspond to the H₄ chain with bond distances $R = 0.9$ Å and $R = 3.4$ Å, respectively. See text for further details.

B. H₈ chain and Helium dimer

We now turn to the longer H₈ chain and the Helium dimer for which the constrained AC has been implemented in the cc-pVDZ basis. As the number of orbitals is too large to perform an exact diagonalization, we used the DMRG method to perform the Lieb maximization and compute the corresponding AC integrand.

For comparison with Pernal's AC formalism [48], we plot in the top panel of Fig. 6 accurate and approximate AC integrands for the stretched H₈ chain with equidistant hydrogen nuclei ($R = 1.8$ Å). Many features that have been discussed previously for the H₄ chain (at equilibrium) are essentially recovered. We note, in particular, the pronounced curvature of the constrained AC integrand that, by construction, PT2 and 1LI completely miss. As shown in Table. II, like in H₄ or the stretched

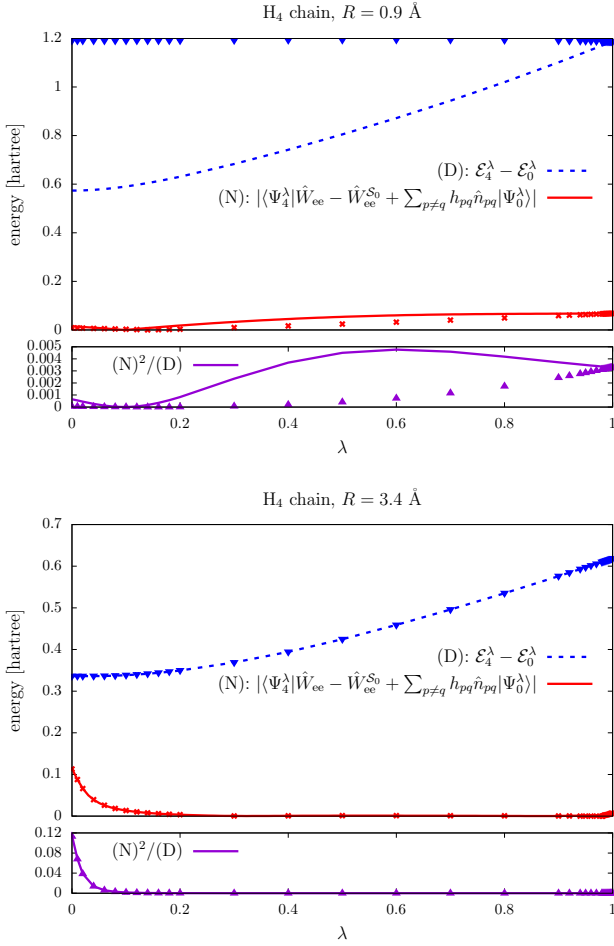


FIG. 5. Same as Fig. 4 for the fourth excited state. Constrained and relaxed AC results are essentially on top of each other when $R = 3.4$ Å (two lower panels).

He₂ molecule (see also the bottom panel of Fig. 6), the former and latter approximations substantially overestimate and underestimate the higher-seniority correlation energy, respectively. As expected, a better description of the constrained AC is obtained at the 2LI level of approximation (see Table. II) or with the PT2-Padé approximant (see Appendix C).

If we relax the constraint on the natural orbital occupations, the curvature of the AC integrand is drastically reduced, like in the H₄ chain at equilibrium, thus leading to a relatively good description of the (relaxed) AC at both PT2 and 1LI levels of approximation. Interestingly, similar features have been reported by Pernal [48] for the stretched H₈ chain within a different AC formalism where, instead, a regular *generalized valence bond* (GVB) wave function is used as reference (see Fig. 2 of Ref. [48]). Still, we note that, for $\lambda = 1$, the relaxed AC integrand is (in absolute value) larger by a factor 3 than that of Pernal. This difference originates from the fact that, in the present (relaxed or constrained)

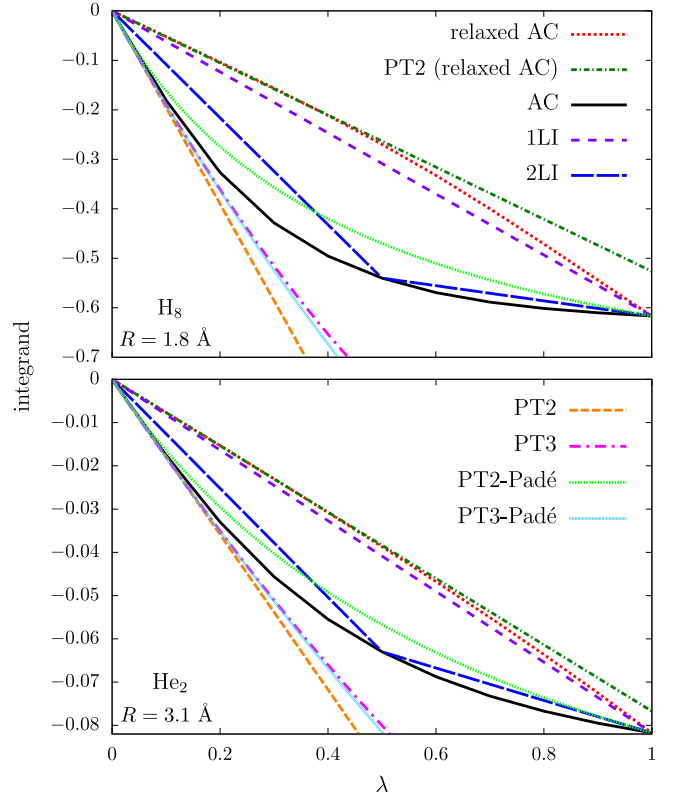


FIG. 6. Constrained and relaxed AC integrands computed at various levels of approximation for the H₈ molecular chain (top panel) and the He₂ molecule (bottom panel). DMRG results (simply referred to as “AC” and “relaxed AC”) are used as reference. Energies are in atomic unit (hartree). For the large interatomic distance $R = 30$ Å, the AC integrand of He₂ is zero (not shown).

AC, the reference ($\lambda = 0$) seniority-zero wave function is constructed from the “exact” physical natural orbitals (*i.e.*, those obtained in the $\lambda = 1$ limit of the AC). Since orbital optimization is of primary importance in variational seniority-zero calculations [71, 76], relaxing the natural orbitals constraint, like in Pernal’s AC [48], would further reduce the higher-seniority correlation energy. The resulting seniority-zero wave function would be optimal energy wise but it would neither reproduce the exact natural orbitals nor their occupancies.

This “dilemma” is also reflected in the stretching energy curves of the Helium dimer (see Fig. 7 and Table III). In comparison with standard DMRG (which gives similar results to FCI [96]), the reference ($\lambda = 0$) seniority-zero calculation of the constrained AC dramatically overbinds: The equilibrium bond distance is underestimated by 0.9 Å and the stretching energy is wrong by a factor 10³. This observation clearly shows the importance of the complementary higher-seniority density-matrix correlation functional in this context. Even though the 2LI approximation recovers a substantial amount of the missing correlation energy

| \overline{W}^S | H ₈ chain ($R = 1.8 \text{ \AA}$) | He ₂ ($R = 3.1 \text{ \AA}$) | H ₄ chain ($R = 0.9 \text{ \AA}$) | H ₄ chain ($R = 3.4 \text{ \AA}$) |
|--|--|---|--|--|
| reference | -0.466432 | -0.055487 | -0.034278 | -0.320665 |
| PT2 | -0.975657(109%) | -0.089689(62%) | -0.054791(60%) | -0.547304(71%) |
| PT3 | -0.702535(51%) | -0.075878(37%) | -0.046463(36%) | -0.433155(35%) |
| PT2-Padé | -0.422700(-9%) | -0.051760(-7%) | -0.031894(-7%) | -0.320182(-0.1%) |
| PT3-Padé | -0.771226(65%) | -0.078647(42%) | -0.047984(40%) | -0.457629(42%) |
| 1LI | -0.308280(-34%) | -0.040870(-26%) | -0.025332(-26%) | -0.255112(-20%) |
| 2LI | -0.424164(-9%) | -0.051930(-6%) | -0.032126(-6%) | -0.309438(-3%) |
| <hr/> | | | | |
| Total energy | | | | |
| Hartree-Fock | -3.817791 | -5.710322 | -2.124260 | -1.268200 |
| $\langle \hat{H} \rangle_{\Psi^{s_0}}$ | -3.663506 | -5.719709 | -2.146038 | -1.545865 |
| DMRG | -4.129982 | -5.775196 | – | – |
| FCI | – | – | -2.180317 | -1.866530 |

TABLE II. Higher-seniority correlation energy \overline{W}^S computed along the constrained AC at various levels of approximation (see Sec. III B) for the H₈ chain, the Helium dimer, and the H₄ chain. Relative deviations from the reference results are given in parentheses. The reference method is DMRG for He₂ and H₈, and FCI for H₄. The total energy using Hartree-Fock, FCI, and DMRG are also reported, together with the expectation value of the Hamiltonian computed with the converged seniority-zero wavefunction.

at equilibrium (see the bottom panel of Fig. 6 and Table II), it fails in describing dynamical correlations at longer bond distances, thus leading to an overestimation by a factor 10^2 of the stretching energy. Better approximations to the higher-seniority correlation energy are definitely needed in this case. For the sake of completeness, we verified numerically that, in the dissociated $R = 30 \text{ \AA}$ geometry, the AC integrand equals zero for all λ values (not shown), as expected for two separate two-electron systems (each of them being described exactly by a seniority-zero wave function). Note that the errors at $\lambda = 0$ (seniority-zero limit) are substantially reduced when switching from the constrained to the relaxed AC, but they remain significant. As expected from the comparison of Table III (see the equilibrium energies) with Fig. 1 of Ref. [96], where the dissociation curve of the Helium dimer has been computed (without BSSE corrections) with a variationally optimized *antisymmetrized product of strongly orthogonal geminals* (APSG), these errors would be further (and drastically) reduced by relaxing, in addition, the natural orbitals constraint. An accurate description of Van der Waals interactions would still require both post-seniority-zero treatment and BSSE corrections [96].

In summary, using as reference a seniority-zero wave function that reproduces the exact 1RDM (by analogy with DFT, where the Kohn-Sham determinant is used for reproducing the exact density) complicates the evaluation of the missing higher-seniority correlation energy, which is substantial, because the corresponding correlation integrand does not vary linearly along the AC.

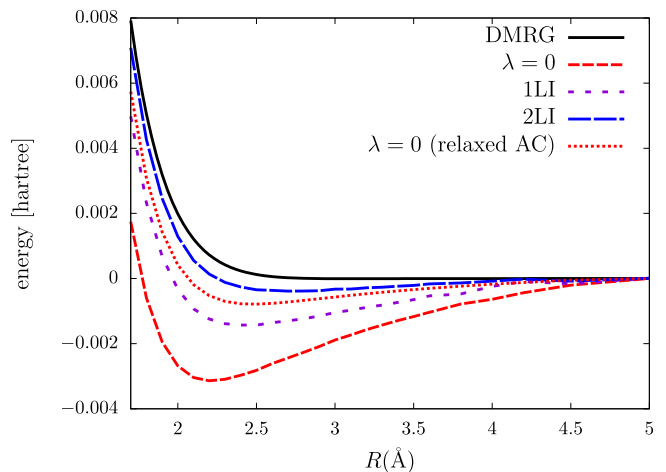


FIG. 7. Stretching energy $E(R) - E(R = 5 \text{ \AA})$ curves of the Helium dimer computed at both seniority-zero ($\lambda = 0$) and higher-seniority (through linear interpolations of the constrained AC integrand) levels of approximation. The relaxed seniority-zero ($\lambda = 0$) curve is shown for analysis purposes. The DMRG curve, which is bound (see Table III), is used as reference. See text for further details.

VI. CONCLUSIONS AND PERSPECTIVES

An alternative exact formulation of RDMFT, where the (one-electron reduced) density matrix is mapped onto an *ab initio* seniority-zero many-body wave function, has been derived. The optimization of both the DOCI coefficients and the natural orbitals has been discussed at the formal level. Exact and approximate adiabatic connection (AC) formulas have been derived and implemented in order to describe the complementary higher-seniority density matrix functional correlation energy. Our proof-of-concept numerical calculations clearly show that relying on a seniority-zero wave

| He ₂ | R_{eq} (Å) | Equilibrium energy | Stretching energy |
|----------------------------|---------------------|--------------------|-------------------|
| $\lambda = 0$ | 2.2 | -5.721112 | 0.003138 |
| $\lambda = 0$ (relaxed AC) | 2.5 | -5.736052 | 0.000786 |
| 1LI | 2.5 | -5.761040 | 0.001440 |
| 2LI | 2.7 | -5.771703 | 0.000395 |
| $\lambda = 1$ (DMRG) | 3.1 | -5.775196 | 0.000006 |

TABLE III. Equilibrium bond distance, total energy at equilibrium, and stretching energy (in Hartree) of the He₂ molecule computed in the cc-pVDZ basis at the constrained and relaxed seniority-zero ($\lambda = 0$) levels of approximation (which is equivalent to perturbation theory through first order) and beyond. In the latter (constrained) case, 1LI and 2LI energy corrections are applied [see Eqs. (86) and (89)]. Comparison is made with DMRG. The stretching energy is evaluated as the difference between the energies at $R = 5$ Å and $R = R_{\text{eq}}$. See text for further details.

function that reproduces the exact density matrix makes the description of higher-seniority correlation energies nontrivial. The latter are indeed substantial in this case, and the corresponding AC integrand has a pronounced curvature. As a result, neither second-order perturbation theory nor a single-segment linear interpolation will be adequate in this context.

In order to turn the present approach into a practical computational method for modelling strongly correlated molecular systems, various practical issues need to be addressed. First of all, one should design density matrix functional approximations to the higher-seniority interaction energy which is obtained by subtracting the seniority-zero density matrix functional energy from the regular full interaction one. The latter might be described with standard functionals, such as the Piris natural orbital functionals (PNOFs) [32, 33], possibly with perturbative corrections [93], in order to fully describe intrapair and interpair correlations. Power-type functionals [20] might also be used, or functionals describing intergeminal correlation effects [133, 137]. Turning to the design of seniority-zero density matrix functional approximations, using the Richardson–Gaudin wave function as a model, as recently proposed by Johnson *et al.* [138], is an appealing idea. In order to evaluate numerically a seniority-zero interaction energy in the present context, the single particle energies would be determined from the orbital occupation constraint while the pairing strength could still be evaluated variationally, like in Ref. 138. Ultimately, we should be able to construct a complementary higher-seniority functional that depends explicitly on the natural orbitals and their occupations, thus allowing for a self-consistent computation of the natural orbitals and the seniority-zero wave function [see Eqs. (49), (50), and (55)]. The challenge, as one follows the above-mentioned strategies, is to ensure that the two (fully and seniority-zero-only interacting) density matrix functional approximations are merged in

a consistent way. For example, using PNOF5 [30] in this context would be irrelevant as it does not include any higher-seniority correlation effect [90, 139]. However, the on-top density functionals used in Refs. 107 and 140 to recover the dynamical correlation missing in the Δ NO approach could be used, as the on-top pair density is expressed as a functional of the natural orbitals and their occupations (see Eq. 34 of Ref. 107). Note also that the resulting higher-seniority functional should in principle vanish in the two-electron case.

Alternatively, a direct computation of the higher-seniority correlation energy, which then becomes an implicit functional of the density matrix, can be performed using the AC formulas in Eqs. (71) and (73). In analogy with recent works by Pernal [48] and then Vu *et al.* [108], the extended random phase approximation could be used for computing AC integrands. One could also follow a different AC path, where the seniority number gradually increases until the full configuration space is covered, in the spirit of Refs 63 and 141. Ideally, the “potential” (*i.e.*, the single particle energies in the AC Hamiltonian) should be adjusted along the AC so that the natural orbital occupation constraint is fulfilled. Note that natural orbitals and occupations could be extracted from a regular (and lower cost) NOFT calculation using PNOFs or power functionals, for example. The above-mentioned implementation schemes should obviously be explored further. This is left for future work.

Finally, the computational burden of performing DOCI calculations within our seniority-zero reformulation of RDMFT can be bypassed by considering recent advances in practical DOCI calculations, such as variational 2RDM-based approximations [108, 142–144], CIPSI [79], FCIQMC solvers [145], a proper choice of Richardson–Gaudin states [146], the pair parametric two-electron reduced density matrix approach [74], or even using quantum computers [147]. One can also truncate the configuration space by considering a maximal degree of excitation [68], or by defining an active space for each electron pair as in the Δ NO method [140]. pCCD and Ap1rog are also appropriate candidates with mean-field cost [62, 69, 70, 72, 73], although they might break down if quadruple excitations are not negligible as they approximate the amplitudes T_4 by T_2^2 .

VII. ACKNOWLEDGMENTS

The authors would like to thank Paul Ayers and Laurent Lemmens for enlightening discussions. They also thank LabEx CSC (grant number: ANR-10-LABX-0026-CSC), IdEx (University of Strasbourg, grant number: W21RPD04), and ANR (grant number: ANR-19-CE07-0024-02 CoLab) for funding. S.Y. acknowledges support from the Interdisciplinary Thematic Institute ITI-CSC

via the IdEx Unistra (ANR-10-IDEX-0002).

Appendix A: Hohenberg–Kohn theorem in the natural orbital space

The natural orbital basis is fixed in the following. Let us consider two potentials $\{\varepsilon_p\}$ and $\{\varepsilon'_p\}$ that differ by more than a constant, and the following *ground-state* seniority-zero interacting Schrödinger equations:

$$\left(\hat{W}_{ee}^{S_0} + \sum_p \varepsilon_p \hat{n}_p \right) |\Psi\rangle = \mathcal{E} |\Psi\rangle, \quad (\text{A.1})$$

and

$$\left(\hat{W}_{ee}^{S_0} + \sum_p \varepsilon'_p \hat{n}_p \right) |\Psi'\rangle = \mathcal{E}' |\Psi'\rangle. \quad (\text{A.2})$$

If we assume that $\Psi = \Psi'$, then it comes from Eqs. (A.1) and (A.2) that

$$\sum_p (\varepsilon'_p - \varepsilon_p) \hat{n}_p |\Psi\rangle = (\mathcal{E}' - \mathcal{E}) |\Psi\rangle. \quad (\text{A.3})$$

The ground-state wave function Ψ can in principle be determined from any seniority-zero Slater determinant Φ_J that overlaps with Ψ through a diffusion process:

$$|\Psi\rangle \sim \lim_{\tau \rightarrow +\infty} e^{-\hat{H}\tau} |\Phi_J\rangle, \quad (\text{A.4})$$

where $\hat{H} = \hat{W}_{ee}^{S_0} + \sum_p \varepsilon_p \hat{n}_p$ is the seniority-zero Hamiltonian in Eq. (A.1). Applying \hat{H} repeatedly (through the exponential) will allow electrons to jump from doubly occupied orbitals in Φ_I to unoccupied ones. Exchange-time-inversion integrals [see Eq. (8)] are central in this process. Thus we deduce the following decomposition:

$$|\Psi\rangle = \sum_{I \in \mathcal{S}_0} C_I |\Phi_I\rangle, \quad (\text{A.5})$$

which is expected to cover the entire seniority-zero subspace. In other words, all C_I coefficients are expected to be non-zero, whatever the index I is. Therefore, inserting Eq. (A.5) into Eq. (A.3) leads to

$$\sum_p (\varepsilon'_p - \varepsilon_p) n_p^{\Phi_I} = (\mathcal{E}' - \mathcal{E}), \forall I, \quad (\text{A.6})$$

where $n_p^{\Phi_I}$ is the occupation of the natural orbital p in Φ_I . If we now assign $N - 2$ electrons to a fixed set of natural orbitals $\{p_i\}_{1 \leq i \leq \frac{N}{2}-1}$ and let the remaining two electrons occupy any other orbital q , it comes from Eq. (A.6):

$$2(\varepsilon'_q - \varepsilon_q) \overset{q \notin \{p_i\}}{\equiv} (\mathcal{E}' - \mathcal{E}) - 2 \sum_{i=1}^{\frac{N}{2}-1} (\varepsilon'_{p_i} - \varepsilon_{p_i}), \quad (\text{A.7})$$

thus leading to

$$\varepsilon'_q - \varepsilon_q \overset{q \notin \{p_i\}}{\equiv} c, \quad (\text{A.8})$$

where c is a constant. As a result, applying Eq. (A.6) to a different situation where none of the $\{p_i\}$ orbitals are occupied leads to

$$\mathcal{E}' - \mathcal{E} = Nc. \quad (\text{A.9})$$

If we now keep only two electrons within the $\{p_i\}$ orbital subspace, while redistributing the remaining $N - 2$ electrons among the other orbitals, we finally obtain from Eqs. (A.6) and (A.8):

$$2(\varepsilon'_q - \varepsilon_q) \overset{q \in \{p_i\}}{\equiv} (\mathcal{E}' - \mathcal{E}) - 2 \left(\frac{N}{2} - 1 \right) c, \quad (\text{A.10})$$

or, equivalently [see Eq. (A.9)],

$$\varepsilon'_q - \varepsilon_q \overset{q \in \{p_i\}}{\equiv} c. \quad (\text{A.11})$$

According to Eqs. (A.8) and (A.11), the two potentials differ by a constant, which is impossible. Therefore $\Psi \neq \Psi'$.

If we now assume, for simplicity, that seniority-zero ground-state energies are not degenerate, then

$$\left\langle \hat{W}_{ee}^{S_0} + \sum_p \varepsilon_p \hat{n}_p \right\rangle_{\Psi} < \left\langle \hat{W}_{ee}^{S_0} + \sum_p \varepsilon_p \hat{n}_p \right\rangle_{\Psi'} \quad (\text{A.12})$$

and

$$\left\langle \hat{W}_{ee}^{S_0} + \sum_p \varepsilon'_p \hat{n}_p \right\rangle_{\Psi'} < \left\langle \hat{W}_{ee}^{S_0} + \sum_p \varepsilon'_p \hat{n}_p \right\rangle_{\Psi} \quad (\text{A.13})$$

according to the Rayleigh–Ritz variational principle. If we assume that Ψ and Ψ' have the same natural orbital occupations, then

$$0 < \left\langle \hat{W}_{ee}^{S_0} \right\rangle_{\Psi} - \left\langle \hat{W}_{ee}^{S_0} \right\rangle_{\Psi'} < 0, \quad (\text{A.14})$$

which is impossible, thus establishing the one-to-one correspondence between the ground-state natural orbital occupations $\{n_p^{\Psi}\}$ and the potential $\{\varepsilon_p\}$.

Appendix B: Stationarity condition for the natural orbitals

The purpose of this appendix is to prove Eq. (55). We start from Eq. (14) whose expansion through first order in the orbital rotation parameters gives

$$\varphi_{p(\boldsymbol{\kappa})}(\mathbf{r}) = \varphi_p(\mathbf{r}) + \sum_q \kappa_{pq} \varphi_q(\mathbf{r}) + \mathcal{O}(\boldsymbol{\kappa}^2), \quad (\text{B.1})$$

or, equivalently,

$$\varphi_{r(\boldsymbol{\kappa})}(\mathbf{r}) = \varphi_r(\mathbf{r}) + \sum_{s < r} \kappa_{rs} \varphi_s(\mathbf{r}) - \sum_{s > r} \kappa_{sr} \varphi_s(\mathbf{r}) + \mathcal{O}(\boldsymbol{\kappa}^2), \quad (\text{B.2})$$

thus leading to

$$\left. \frac{\partial \varphi_{r(\kappa)}(\mathbf{r})}{\partial \kappa_{pq}} \right|_{\kappa=0} = \delta_{rp} \varphi_q(\mathbf{r}) - \delta_{rq} \varphi_p(\mathbf{r}). \quad (\text{B.3})$$

As a result, the first term on the left-hand side of Eq. (54) can be written as follows [see Eq. (42)]:

$$\begin{aligned} & \left. (\partial \mathbf{h}(\kappa) / \partial \kappa_{pq} | \mathbf{n}^{\Psi^{S_0}}) \right|_{\kappa=0} \\ &= 2 \sum_r \langle \varphi_r | \hat{h} | \partial \varphi_{r(\kappa)} / \partial \kappa_{pq} \rangle \Big|_{\kappa=0} n_r^{\Psi^{S_0}} \\ &= 2h_{pq} (n_p^{\Psi^{S_0}} - n_q^{\Psi^{S_0}}). \end{aligned} \quad (\text{B.4})$$

Turning to the second term on the left-hand side of Eq. (54), we may rewrite the expectation value for the seniority-zero interaction as [see Eq. (29)]

$$\begin{aligned} \langle \Psi^{S_0} | \hat{W}_{ee}^{S_0}(\kappa) | \Psi^{S_0} \rangle &= \frac{1}{2} \sum_{p \neq q} \langle pq | pq \rangle^\kappa \langle \hat{n}_p \hat{n}_q \rangle_{\Psi^{S_0}} \\ &- \frac{1}{2} \sum_{p \neq q} \sum_{\sigma} \langle pq | qp \rangle^\kappa \langle \hat{n}_{p\sigma} \hat{n}_{q\sigma} \rangle_{\Psi^{S_0}} \\ &+ \sum_{pq} \langle pp | qq \rangle^\kappa \langle \hat{P}_p^\dagger \hat{P}_q \rangle_{\Psi^{S_0}}, \end{aligned} \quad (\text{B.5})$$

or, equivalently [we use the simplified expression $\langle \hat{n}_{p\sigma} \hat{n}_{q\sigma'} \rangle_{\Psi^{S_0}} = (1/4) \langle \hat{n}_p \hat{n}_q \rangle_{\Psi^{S_0}}$ which holds for seniority-zero wave functions],

$$\begin{aligned} & \langle \Psi^{S_0} | \hat{W}_{ee}^{S_0}(\kappa) | \Psi^{S_0} \rangle \\ &= \frac{1}{4} \sum_{rs} [2 \langle rs | rs \rangle^\kappa - \langle rs | sr \rangle^\kappa] (1 - \delta_{rs}) \langle \hat{n}_r \hat{n}_s \rangle_{\Psi^{S_0}} \\ &+ \sum_{rs} \langle rr | ss \rangle^\kappa \langle \hat{P}_r^\dagger \hat{P}_s \rangle_{\Psi^{S_0}} \\ &= \frac{1}{4} \sum_{rs} [2 \langle rs | rs \rangle^\kappa - \langle rs | sr \rangle^\kappa] \langle \hat{n}_r \hat{n}_s \rangle_{\Psi^{S_0}} \\ &+ \sum_{rs} \langle rr | ss \rangle^\kappa (1 - \delta_{rs}) \langle \hat{P}_r^\dagger \hat{P}_s \rangle_{\Psi^{S_0}}, \end{aligned} \quad (\text{B.6})$$

where we used the fact that $\langle \hat{P}_r^\dagger \hat{P}_r \rangle_{\Psi^{S_0}} = \frac{1}{4} \langle \hat{n}_r \hat{n}_r \rangle_{\Psi^{S_0}}$. Since, according to Eq. (B.3),

$$\begin{aligned} \frac{1}{2} \partial \langle rs | rs \rangle^\kappa / \partial \kappa_{pq} \Big|_{\kappa=0} &= \delta_{rp} \langle qs | rs \rangle - \delta_{rq} \langle ps | rs \rangle \\ &+ \delta_{sp} \langle rq | rs \rangle - \delta_{sq} \langle rp | rs \rangle, \end{aligned} \quad (\text{B.7})$$

$$\begin{aligned} \frac{1}{2} \partial \langle rs | sr \rangle^\kappa / \partial \kappa_{pq} \Big|_{\kappa=0} &= \delta_{rp} \langle qs | sr \rangle - \delta_{rq} \langle ps | sr \rangle \\ &+ \delta_{sp} \langle rq | sr \rangle - \delta_{sq} \langle rp | sr \rangle, \end{aligned} \quad (\text{B.8})$$

and

$$\begin{aligned} \frac{1}{2} \partial \langle rr | ss \rangle^\kappa / \partial \kappa_{pq} \Big|_{\kappa=0} &= \delta_{rp} \langle qr | ss \rangle - \delta_{rq} \langle pr | ss \rangle \\ &+ \delta_{sp} \langle rr | qs \rangle - \delta_{sq} \langle rr | ps \rangle, \end{aligned} \quad (\text{B.9})$$

we obtain from Eq. (B.6):

$$\begin{aligned} & \langle \Psi^{S_0} | \partial \hat{W}_{ee}^{S_0}(\kappa) / \partial \kappa_{pq} | \Psi^{S_0} \rangle \Big|_{\kappa=0} \\ &= \sum_r [2 \langle rp | rq \rangle - \langle rp | qr \rangle] [\langle \hat{n}_r \hat{n}_p \rangle_{\Psi^{S_0}} - \langle \hat{n}_r \hat{n}_q \rangle_{\Psi^{S_0}}] \\ &+ 4 \sum_r \langle pq | rr \rangle \\ &\times \left[(1 - \delta_{rp}) \langle \hat{P}_r^\dagger \hat{P}_p \rangle_{\Psi^{S_0}} - (1 - \delta_{rq}) \langle \hat{P}_r^\dagger \hat{P}_q \rangle_{\Psi^{S_0}} \right]. \end{aligned} \quad (\text{B.10})$$

Finally, by expressing the third term on the left-hand side of Eq. (54) as follows:

$$\begin{aligned} & \left. \frac{\partial \overline{W}^S(\kappa, \mathbf{n}^{\Psi^{S_0}})}{\partial \kappa_{pq}} \right|_{\kappa=0} = \left. \frac{\partial \overline{W}^S(\{\varphi_{r(\kappa)}\}, \mathbf{n}^{\Psi^{S_0}})}{\partial \kappa_{pq}} \right|_{\kappa=0} \\ &= \sum_r \int d\mathbf{r} \left. \frac{\partial \varphi_{r(\kappa)}(\mathbf{r})}{\partial \kappa_{pq}} \right|_{\kappa=0} \frac{\delta \overline{W}^S(\{\varphi_r\}, \mathbf{n}^{\Psi^{S_0}})}{\delta \varphi_r(\mathbf{r})} \\ &\equiv \sum_r \left\langle \left. \frac{\partial \varphi_{r(\kappa)}(\mathbf{r})}{\partial \kappa_{pq}} \right|_{\kappa=0} \left| \frac{\delta \overline{W}^S(\{\varphi_r\}, \mathbf{n}^{\Psi^{S_0}})}{\delta \varphi_r} \right. \right\rangle \\ &= \left\langle \varphi_q \left| \frac{\delta \overline{W}^S(\{\varphi_p\}, \mathbf{n}^{\Psi^{S_0}})}{\delta \varphi_p} \right. \right\rangle \\ &- \left\langle \varphi_p \left| \frac{\delta \overline{W}^S(\{\varphi_q\}, \mathbf{n}^{\Psi^{S_0}})}{\delta \varphi_q} \right. \right\rangle, \end{aligned} \quad (\text{B.11})$$

we recover Eq. (55) from Eqs. (B.4), (B.10), (54) and (56).

Appendix C: PT2/PT3-based Padé approximants to the AC integrand

By analogy with the interaction-strength interpolation schemes that have been developed in the context of DFT [121, 148–152], we propose two PT-based Padé approximants to the AC integrand. In the first one, which is referred to as PT2-Padé approximant and reads

$$\begin{aligned} \overline{W}^{S,\lambda} \text{PT2-Padé} &\approx \frac{\mathcal{W}_1 \mathcal{W}^{\lambda=1}}{\mathcal{W}^{\lambda=1} - \mathcal{W}_1} \\ &\times \left(1 - \frac{1}{1 - \frac{(\mathcal{W}^{\lambda=1} - \mathcal{W}_1)_\lambda}{\mathcal{W}^{\lambda=1}}} \right), \end{aligned} \quad (\text{C.1})$$

where we denote $\mathcal{W}^{\lambda=1} = \overline{W}^{S,\lambda=1}$ and $\mathcal{W}_1 = \partial \overline{W}^{S,\lambda} / \partial \lambda \Big|_{\lambda=0}$, the $\lambda \rightarrow 0$ and $\lambda \rightarrow 1$ limits of the AC integrand are described exactly through first order (in λ) and zeroth order (in $\lambda - 1$), respectively. At this level of approximation, the energy (which is obtained after integration over λ) is exact through

second order in λ , hence the name of the approximant.

The second approximant, which is referred to as PT3-Padé and relies exclusively on the $\lambda \rightarrow 0$ limit of the AC, reads

$$\overline{\mathcal{W}}^{S,\lambda} \stackrel{\text{PT3-Padé}}{\approx} -\frac{\mathcal{W}_1^2}{\mathcal{W}_2} \left(1 - \frac{1}{1 - \frac{\mathcal{W}_2}{\mathcal{W}_1} \lambda} \right), \quad (\text{C.2})$$

where $\mathcal{W}_2 = \frac{1}{2} \partial^2 \overline{\mathcal{W}}^{S,\lambda} / \partial \lambda^2 \Big|_{\lambda=0}$. It reproduces the correct expansion of the integrand through second order in λ ,

$$\overline{\mathcal{W}}^{S,\lambda} \stackrel{\text{PT3}}{\approx} \lambda \mathcal{W}_1 + \lambda^2 \mathcal{W}_2, \quad (\text{C.3})$$

and therefore is exact through third order in λ for the energy (after integration over λ),

$$E \stackrel{\text{PT3}}{\approx} \langle \hat{H} \rangle_{\Psi_{S_0}} + \frac{1}{2} \mathcal{W}_1 + \frac{1}{3} \mathcal{W}_2, \quad (\text{C.4})$$

hence the name of the approximant. For completeness, we derived the PT2-Padé and PT3-Padé energies, that read

$$E \stackrel{\text{PT2-Padé}}{\approx} \langle \hat{H} \rangle_{\Psi_{S_0}} - \frac{\mathcal{W}_1 \mathcal{W}^{\lambda=1}}{\mathcal{W}^{\lambda=1} - \mathcal{W}_1} - \frac{\mathcal{W}_1 (\mathcal{W}^{\lambda=1})^2}{(\mathcal{W}^{\lambda=1} - \mathcal{W}_1)^2} \ln \left| 1 - \frac{\mathcal{W}^{\lambda=1} - \mathcal{W}_1}{\mathcal{W}^{\lambda=1}} \right| \quad (\text{C.5})$$

and

$$E \stackrel{\text{PT3-Padé}}{\approx} \langle \hat{H} \rangle_{\Psi_{S_0}} - \frac{\mathcal{W}_1^2}{\mathcal{W}_2} - \frac{\mathcal{W}_1^3}{\mathcal{W}_2^2} \ln \left| 1 - \frac{\mathcal{W}_2}{\mathcal{W}_1} \right|. \quad (\text{C.6})$$

In the present work, \mathcal{W}_1 and \mathcal{W}_2 have been evaluated numerically, for analysis purposes. In practice, exact analytical expressions might be used instead [see Eq. (83) for \mathcal{W}_1]. Regarding \mathcal{W}_2 , according to Eqs. (60) and (82), we have

$$\frac{1}{2} \frac{\partial^2 \overline{\mathcal{W}}^{S,\lambda}}{\partial \lambda^2} = \langle \hat{\nu}^\lambda \rangle_{\frac{\partial \Psi_0^\lambda}{\partial \lambda}} + \left\langle \Psi_0^\lambda \left| \hat{\nu}^\lambda \left| \frac{\partial^2 \Psi_0^\lambda}{\partial \lambda^2} \right. \right. \right\rangle + \left\langle \Psi_0^\lambda \left| \frac{\partial^2 \hat{\varepsilon}^\lambda}{\partial \lambda^2} \left| \frac{\partial \Psi_0^\lambda}{\partial \lambda} \right. \right. \right\rangle, \quad (\text{C.7})$$

where we used the shorthand notations $\hat{\nu}^\lambda = \hat{\nu} + \frac{\partial \hat{\varepsilon}^\lambda}{\partial \lambda}$ and $\hat{\varepsilon}^\lambda = \sum_p \varepsilon_p^\lambda \hat{n}_p$. Since the last term on the right-hand side of Eq. (C.7) vanishes, according to the natural orbital occupations constraint,

$$2 \left\langle \Psi_0^\lambda \left| \frac{\partial^2 \hat{\varepsilon}^\lambda}{\partial \lambda^2} \left| \frac{\partial \Psi_0^\lambda}{\partial \lambda} \right. \right. \right\rangle = \sum_p \frac{\partial^2 \varepsilon_p^\lambda}{\partial \lambda^2} \frac{\partial \langle \hat{n}_p \rangle_{\Psi_0^\lambda}}{\partial \lambda} = 0, \quad (\text{C.8})$$

the second-order derivative of the constrained AC integrand can be written more explicitly in perturbation theory as follows [153],

$$\begin{aligned} \frac{1}{6} \frac{\partial^2 \overline{\mathcal{W}}^{S,\lambda}}{\partial \lambda^2} = & \sum_{I>0} \sum_{J>0} \frac{\langle \Psi_0^\lambda | \hat{\nu}^\lambda | \Psi_J^\lambda \rangle \langle \Psi_J^\lambda | \hat{\nu}^\lambda | \Psi_I^\lambda \rangle \langle \Psi_I^\lambda | \hat{\nu}^\lambda | \Psi_0^\lambda \rangle}{(\varepsilon_0^\lambda - \varepsilon_I^\lambda)(\varepsilon_0^\lambda - \varepsilon_J^\lambda)} \\ & - \langle \Psi_0^\lambda | \hat{\nu}^\lambda | \Psi_0^\lambda \rangle \sum_{I>0} \frac{|\langle \Psi_0^\lambda | \hat{\nu}^\lambda | \Psi_I^\lambda \rangle|^2}{(\varepsilon_0^\lambda - \varepsilon_I^\lambda)^2} \\ & + \frac{1}{3} \sum_{I>0} \frac{\langle \Psi_0^\lambda | \hat{\nu}^\lambda | \Psi_I^\lambda \rangle \langle \Psi_I^\lambda | \left(\frac{\partial^2 \hat{\varepsilon}^\lambda}{\partial \lambda^2} \right) | \Psi_0^\lambda \rangle}{\varepsilon_0^\lambda - \varepsilon_I^\lambda}. \end{aligned} \quad (\text{C.9})$$

Note that the last term on the right-hand side of Eq. (C.9) originates from the fact that, unlike in regular perturbation theory, the perturbation operator contains second- (and higher-) order contributions [153–155]:

$$\begin{aligned} (\lambda + \delta) \hat{\nu} + \hat{\varepsilon}^{\lambda+\delta} = & \lambda \hat{\nu} + \hat{\varepsilon}^\lambda + \delta \hat{\nu}^\lambda \\ & + \frac{\delta^2}{2} \frac{\partial^2 \hat{\varepsilon}^\lambda}{\partial \lambda^2} + \mathcal{O}(\delta^3). \end{aligned} \quad (\text{C.10})$$

When rewritten as follows in terms of the first-order wave function, it actually cancels out, as readily seen from Eq. (C.8):

$$\frac{1}{3} \left\langle \frac{\partial \Psi_0^\lambda}{\partial \lambda} \left| \left(\frac{\partial^2 \hat{\varepsilon}^\lambda}{\partial \lambda^2} \right) \right| \Psi_0^\lambda \right\rangle = 0. \quad (\text{C.11})$$

As a result, \mathcal{W}_2 can be evaluated exactly solely from the first-order wave function, like in regular PT3:

$$\frac{1}{6} \frac{\partial^2 \overline{\mathcal{W}}^{S,\lambda}}{\partial \lambda^2} = \langle \hat{\nu}^\lambda \rangle_{\frac{\partial \Psi_0^\lambda}{\partial \lambda}} - \langle \hat{\nu}^\lambda \rangle_{\Psi_0^\lambda} \left\langle \frac{\partial \Psi_0^\lambda}{\partial \lambda} \left| \frac{\partial \Psi_0^\lambda}{\partial \lambda} \right. \right\rangle \quad (\text{C.12})$$

Appendix D: Convergence of the DMRG energy

The DMRG sweep energy for a given number of renormalized states m has a convergence criterion of 10^{-10} Eh. To assess the convergence with respect to m , we did several calculations for different values of m reported in Table D. According to Table D, $m = 400$ is more than enough for the Helium dimer, for which even 20 states are sufficient. For H_8 in the cc-pVDZ basis, the DMRG energy is converged up to 10^{-5} Hartree at $m = 800$, which we considered large enough to neglect the effect of orbital ordering.

Appendix E: First- and second-order derivatives of the correlation integrand

The first-order derivative of the correlation integrand at $\lambda = 0$ is required to compute the energy in the PT3

TABLE D. DMRG energy in Hartree with respect to the number of renormalized states m .

| H_8 | $(R = 1.8 \text{ \AA})$ | He_2 | $(R = 3.1 \text{ \AA})$ |
|-------|-------------------------|--------|-------------------------|
| m | DMRG energy | m | DMRG energy |
| 100 | -4.125716 | 20 | -5.775195 |
| 200 | -4.129171 | 40 | -5.775195 |
| 300 | -4.129746 | 100 | -5.775195 |
| 400 | -4.129900 | 200 | -5.775195 |
| 500 | -4.129949 | 300 | -5.775195 |
| 600 | -4.129969 | 400 | -5.775195 |
| 700 | -4.129978 | | |
| 800 | -4.129982 | | |
| 1200 | -4.129985 | | |
| 1600 | -4.129986 | | |

TABLE E. Parameters (in Hartree) obtained by fitting the correlation integrand with the polynomial $a\lambda^2 + b\lambda$ in between $\lambda = 0$ and $\lambda = 0.2$.

| System | a | b |
|----------------------------------|-----------|-----------|
| H_4 ($R = 0.9 \text{ \AA}$) | 0.0572817 | -0.112019 |
| H_4 ($R = 3.4 \text{ \AA}$) | 0.74256 | -1.11383 |
| He_2 ($R = 3.1 \text{ \AA}$) | 0.0997618 | -0.185009 |
| H_8 ($R = 1.8 \text{ \AA}$) | 1.7061 | -1.97377 |

and PT2-Padé approximations, in addition to the second-order derivative at $\lambda = 0$ for the PT3-Padé approximations. They have been estimated by fitting the correlation integrand using the implementation of the nonlinear least-squares Marquardt-Levenberg algorithm in gnuplot, in between $\lambda = 0$ and $\lambda = 0.2$. A polynomial of degree 2, i.e. $a\lambda^2 + b\lambda$, has been considered such that

$$\left. \frac{\partial \overline{\mathcal{W}}^{S,\lambda}}{\partial \lambda} \right|_{\lambda=0} = b, \quad (\text{E.1})$$

and

$$\left. \frac{\partial^2 \overline{\mathcal{W}}^{S,\lambda}}{\partial \lambda^2} \right|_{\lambda=0} = a. \quad (\text{E.2})$$

The values of a and b are reported in Table E.

- [1] A. D. Becke, *J. Chem. Phys.* **138**, 074109 (2013).
- [2] C. J. Stein, V. von Burg, and M. Reiher, *J. Chem. Theory Comput.* **12**, 3764 (2016).
- [3] T. Helgaker, P. Jorgensen, and J. Olsen, *Molecular electronic-structure theory* (John Wiley & Sons, 2014).
- [4] R. J. Bartlett and M. Musiał, *Rev. Mod. Phys.* **79**, 291 (2007).
- [5] D. I. Lyakh, M. Musiał, V. F. Lotrich, and R. J. Bartlett, *Chem. Rev.* **112**, 182 (2011).
- [6] P. Hohenberg and W. Kohn, *Phys. Rev.* **136**, B864 (1964).
- [7] W. Kohn and L. Sham, *Phys. Rev.* **140**, A1133 (1965).
- [8] A. J. Cohen, P. Mori-Sánchez, and W. Yang, *Chem. Rev.* **112**, 289 (2011).
- [9] M. Swart, *Int. J. Quantum Chem.* **113**, 2 (2013).
- [10] M. Swart and M. Gruden, *Acc. Chem. Res.* **49**, 2690 (2016).
- [11] T. L. Gilbert, *Phys. Rev. B* **12**, 2111 (1975).
- [12] R. A. Donnelly and R. G. Parr, *J. Chem. Phys.* **69**, 4431 (1978).
- [13] R. A. Donnelly, *J. Chem. Phys.* **71**, 2874 (1979).
- [14] K. Pernal and K. J. Giesbertz, in *Density-Functional Methods for Excited States* (Springer, 2015) pp. 125–183.
- [15] A. Müller, *Phys. Lett. A* **105**, 446 (1984).
- [16] S. Goedecker and C. Umrigar, *Phys. Rev. Lett.* **81**, 866 (1998).
- [17] A. Holas, *Phys. Rev. A* **59**, 3454 (1999).
- [18] M. A. Buijse and E. J. Baerends, *Mol. Phys.* **100**, 401 (2002).
- [19] O. Gritsenko, K. Pernal, and E. J. Baerends, *J. Chem. Phys.* **122**, 204102 (2005).
- [20] S. Sharma, J. K. Dewhurst, N. N. Lathiotakis, and E. K. U. Gross, *Phys. Rev. B* **78**, 201103 (2008).
- [21] N. N. Lathiotakis, S. Sharma, J. K. Dewhurst, F. G. Eich, M. A. L. Marques, and E. K. U. Gross, *Phys. Rev. A* **79**, 040501 (2009).
- [22] N. N. Lathiotakis, N. Helbig, A. Zacarias, and E. K. U. Gross, *J. Chem. Phys.* **130**, 064109 (2009).
- [23] M. A. Marques and N. Lathiotakis, *Phys. Rev. A* **77**, 032509 (2008).
- [24] M. Rodríguez-Mayorga, E. Ramos-Cordoba, M. Vianadal, M. Piris, and E. Matito, *Phys. Chem. Chem. Phys.* **19**, 24029 (2017).
- [25] M. Piris and P. Otto, *Int. J. Quantum Chem.* **94**, 317 (2003).
- [26] P. Leiva and M. Piris, *J. Mol. Struct. THEOCHEM* **719**, 63 (2005).
- [27] M. Piris, *Int. J. Quantum Chem.* **106**, 1093 (2006).
- [28] M. Piris, X. Lopez, and J. Ugalde, *J. Chem. Phys.* **126**, 214103 (2007).
- [29] M. Piris and J. M. Ugalde, *J. Comput. Chem.* **30**, 2078 (2009).
- [30] M. Piris, X. Lopez, F. Ruipérez, J. Matxain, and J. Ugalde, *J. Chem. Phys.* **134**, 164102 (2011).
- [31] M. Piris, *Int. J. Quantum Chem.* **113**, 620 (2013).
- [32] M. Piris, *J. Chem. Phys.* **141**, 044107 (2014).
- [33] M. Piris and J. M. Ugalde, *Int. J. Quantum Chem.* **114**, 1169 (2014).
- [34] E. Ramos-Cordoba, X. Lopez, M. Piris, and E. Matito, *J. Chem. Phys.* **143**, 164112 (2015).
- [35] X. Lopez, M. Piris, F. Ruipérez, and J. M. Ugalde, *J. Phys. Chem. A* **119**, 6981 (2015).
- [36] I. Mitxelena, M. Piris, and M. Rodríguez-Mayorga, *J. Phys. Condens. Matter* **29**, 425602 (2017).
- [37] A. Savin, *Recent Developments and Applications of Modern Density Functional Theory* (Elsevier, Amsterdam, 1996) p. 327.
- [38] J. Toulouse, F. Colonna, and A. Savin, *Phys. Rev. A* **70**, 062505 (2004).
- [39] E. Fromager, *Mol. Phys.* **113**, 419 (2015).
- [40] B. Senjean, *Phys. Rev. B* **100**, 035136 (2019).
- [41] F. Libisch, C. Huang, and E. A. Carter, *Acc. Chem. Res.* **47**, 2768 (2014).
- [42] G. Li Manni, R. K. Carlson, S. Luo, D. Ma, J. Olsen, D. G. Truhlar, and L. Gagliardi, *J. Chem. Theory Comput.* **10**, 3669 (2014).
- [43] L. Gagliardi, D. G. Truhlar, G. Li Manni, R. K. Carlson, C. E. Hoyer, and J. L. Bao, *Acc. Chem. Res.* **50**, 66 (2016).
- [44] M. Mostafanejad and A. E. DePrince III, *J. Chem. Theory Comput.* **15**, 290 (2018).
- [45] M. Mostafanejad, M. D. Liebenthal, and A. E. DePrince III, *J. Chem. Theory Comput.* **16**, 2274 (2020).
- [46] S. J. Lee, M. Welborn, F. R. Manby, and T. F. Miller III, *Acc. Chem. Res.* **52**, 1359 (2019).
- [47] M. A. Mosquera, L. O. Jones, C. H. Borca, M. A. Ratner, and G. C. Schatz, *J. Phys. Chem. A* **123**, 4785 (2019).
- [48] K. Pernal, *Phys. Rev. Lett.* **120**, 013001 (2018).
- [49] K. Pernal, *J. Chem. Phys.* **149**, 204101 (2018).
- [50] E. Pastorczak, M. Hapka, L. Veis, and K. Pernal, *J. Phys. Chem. Lett.* **10**, 4668 (2019).
- [51] E. Maradzike, M. Hapka, K. Pernal, and A. E. DePrince, *J. Chem. Theory Comput.* (2020).
- [52] D. Drwal, P. Beran, M. Hapka, M. Modrzejewski, A. Sokół, L. Veis, and K. Pernal, *arXiv:2204.02340* (2022).
- [53] L. N. Bardeen, L. N. Cooper, and J. R. Schrieffer, *Phys. Rev.* **108**, 1175 (1957).
- [54] A. C. Hurley, J. E. Lennard-Jones, and J. A. Pople, *Proc. R. Soc. Lond. A* **220**, 446 (1953).
- [55] W. Kutzelnigg, *J. Chem. Phys.* **40**, 3640 (1964).
- [56] A. J. Coleman, *J. Math. Phys.* **6**, 1425 (1965).
- [57] D. M. Silver, *J. Chem. Phys.* **50**, 5108 (1969).
- [58] P. R. Surján, in *Correlation and localization* (Springer, 1999) p. 63.
- [59] V. A. Rassolov, *J. Chem. Phys.* **117**, 5978 (2002).
- [60] P. R. Surján, in *Reference Module in Chemistry, Molecular Sciences and Chemical Engineering* (Elsevier, 2016).
- [61] C.-É. Fecteau, F. Berthiaume, M. Khalfoun, and P. A. Johnson, *J. Math. Chem.* **59**, 289 (2021).
- [62] P. A. Johnson, P. W. Ayers, P. A. Limacher, S. De Baerdemacker, D. Van Neck, and P. Bultinck, *Comp. Theor. Chem.* **1003**, 101 (2013).
- [63] L. Bytautas, T. M. Henderson, C. A. Jiménez-Hoyos, J. K. Ellis, and G. E. Scuseria, *J. Chem. Phys.* **135**, 044119 (2011).
- [64] L. Bytautas and J. Dukelsky, *Comput. Theor. Chem.* **1141**, 74 (2018).

- [65] F. Weinhold and E. B. Wilson Jr, *J. Chem. Phys.* **46**, 2752 (1967).
- [66] P. A. Limacher, *J. Chem. Phys.* **145**, 194102 (2016).
- [67] K. Gunst, D. Van Neck, P. A. Limacher, and S. De Baerdemacker, *SciPost Chemistry* **1**, 001 (2021).
- [68] F. Kossoski, Y. Damour, and P.-F. Loos, *J. Phys. Chem. Lett.* **13**, 4342 (2022).
- [69] P. A. Limacher, P. W. Ayers, P. A. Johnson, S. De Baerdemacker, D. Van Neck, and P. Bultinck, *J. Chem. Theory Comput.* **9**, 1394 (2013).
- [70] P. Tecmer, K. Boguslawski, P. A. Johnson, P. A. Limacher, M. Chan, T. Verstraelen, and P. W. Ayers, *J. Phys. Chem. A* **118**, 9058 (2014).
- [71] K. Boguslawski, P. Tecmer, P. W. Ayers, P. Bultinck, S. De Baerdemacker, and D. Van Neck, *Phys. Rev. B* **89**, 201106 (2014).
- [72] T. Stein, T. M. Henderson, and G. E. Scuseria, *J. Chem. Phys.* **140**, 214113 (2014).
- [73] T. M. Henderson, I. W. Bulik, and G. E. Scuseria, *J. Chem. Phys.* **142**, 214116 (2015).
- [74] N. Vu and A. E. DePrince III, *J. Chem. Phys.* **152**, 244103 (2020).
- [75] K. Boguslawski, *Chem. Commun.* **57**, 12277 (2021).
- [76] P. A. Limacher, T. D. Kim, P. W. Ayers, P. A. Johnson, S. De Baerdemacker, D. Van Neck, and P. Bultinck, *Mol. Phys.* **112**, 853 (2014).
- [77] K. Boguslawski, P. Tecmer, P. Bultinck, S. De Baerdemacker, D. Van Neck, and P. W. Ayers, *J. Chem. Theory Comput.* **10**, 4873 (2014).
- [78] K. Boguslawski, P. Tecmer, P. A. Limacher, P. A. Johnson, P. W. Ayers, P. Bultinck, S. De Baerdemacker, and D. Van Neck, *J. Chem. Phys.* **140**, 214114 (2014).
- [79] F. Kossoski, A. Marie, A. Scemama, M. Caffarel, and P.-F. Loos, *J. Chem. Theory Comput.* **17**, 4756 (2021).
- [80] A. Marie, F. Kossoski, and P.-F. Loos, *J. Chem. Phys.* **155**, 104105 (2021).
- [81] K. Boguslawski, *J. Chem. Phys.* **145**, 234105 (2016).
- [82] K. Boguslawski, *J. Chem. Theory Comput.* **15**, 18 (2018).
- [83] K. Boguslawski, P. Tecmer, and Ö. Legeza, *Phys. Rev. B* **94**, 155126 (2016).
- [84] I. Røeggen, in *Correlation and Localization* (Springer, 1999) pp. 89–103.
- [85] E. Rosta and P. Surján, *Int. J. Quantum Chem.* **80**, 96 (2000).
- [86] E. Rosta and P. R. Surján, *J. Chem. Phys.* **116**, 878 (2002).
- [87] V. A. Rassolov, F. Xu, and S. Garashchuk, *J. Chem. Phys.* **120**, 10385 (2004).
- [88] M. Kobayashi, Á. Szabados, H. Nakai, and P. R. Surján, *J. Chem. Theory Comput.* **6**, 2024 (2010).
- [89] M. Tarumi, M. Kobayashi, and H. Nakai, *J. Chem. Theory Comput.* **8**, 4330 (2012).
- [90] M. Piris, *J. Chem. Phys.* **139**, 064111 (2013).
- [91] P. A. Limacher, *J. Chem. Theory Comput.* **11**, 3629 (2015).
- [92] K. Boguslawski and P. Tecmer, *J. Chem. Theory Comput.* **13**, 5966 (2017).
- [93] M. Piris, *Phys. Rev. Lett.* **119**, 063002 (2017).
- [94] F. Brzek, K. Boguslawski, P. Tecmer, and P. S. Zuchowski, *J. Chem. Theory Comput.* **15**, 4021 (2019).
- [95] W. Kutzelnigg, *Chem. Phys.* **401**, 119 (2012).
- [96] T. Zoboki, Á. Szabados, and P. R. Surján, *J. Chem. Theory Comput.* **9**, 2602 (2013).
- [97] J. W. Hollett and P.-F. Loos, *J. Chem. Phys.* **152**, 014101 (2020).
- [98] Á. Margócsy and Á. Szabados, *Theor. Chem. Acc.* **139**, 1 (2020).
- [99] A. Nowak, Ö. Legeza, and K. Boguslawski, *J. Chem. Phys.* **154**, 084111 (2021).
- [100] T. M. Henderson, I. W. Bulik, T. Stein, and G. E. Scuseria, *J. Chem. Phys.* **141**, 244104 (2014).
- [101] K. Boguslawski and P. W. Ayers, *J. Chem. Theory Comput.* **11**, 5252 (2015).
- [102] A. Leszczyk, M. Máté, O. Legeza, and K. Boguslawski, *J. Chem. Theory Comput.* **18**, 96 (2021).
- [103] K. Pernal, *J. Chem. Theory Comput.* **10**, 4332 (2014).
- [104] Á. Margócsy, P. Kowalski, K. Pernal, and Á. Szabados, *Theor. Chem. Acc.* **137**, 159 (2018).
- [105] A. J. Garza, I. W. Bulik, T. M. Henderson, and G. E. Scuseria, *J. Chem. Phys.* **142**, 044109 (2015).
- [106] A. J. Garza, I. W. Bulik, T. M. Henderson, and G. E. Scuseria, *Phys. Chem. Chem. Phys.* **17**, 22412 (2015).
- [107] J. W. Hollett, H. Hosseini, and C. Menzies, *J. Chem. Phys.* **145**, 084106 (2016).
- [108] N. Vu, I. Mitxelena, and A. E. DePrince III, *J. Chem. Phys.* **151**, 244121 (2019).
- [109] T. M. Henderson and G. E. Scuseria, *J. Chem. Phys.* **151**, 051101 (2019).
- [110] T. M. Henderson and G. E. Scuseria, *J. Chem. Phys.* **153**, 084111 (2020).
- [111] R. Dutta, T. M. Henderson, and G. E. Scuseria, *J. Chem. Theory Comput.* **16**, 6358 (2020).
- [112] A. Khamoshi, G. P. Chen, T. M. Henderson, and G. E. Scuseria, *J. Chem. Phys.* **154**, 074113 (2021).
- [113] A. Khamoshi, F. A. Evangelista, and G. E. Scuseria, *Quantum Sci. Technol.* **6**, 014004 (2020).
- [114] P.-O. Löwdin and H. Shull, *Phys. Rev.* **101**, 1730 (1956).
- [115] L. M. Mentel, R. van Meer, O. V. Gritsenko, and E. J. Baerends, *J. Chem. Phys.* **140**, 214105 (2014).
- [116] K. Capelle and V. L. Campo Jr., *Phys. Rep.* **528**, 91 (2013).
- [117] M. Levy, *Proc. Natl. Acad. Sci.* **76**, 6062 (1979).
- [118] B. Senjean, N. Nakatani, M. Tsuchiizu, and E. Fromager, *Phys. Rev. B* **97**, 235105 (2018).
- [119] E. H. Lieb, *Int. J. Quantum Chem.* **24**, 243 (1983).
- [120] Y. Cornaton, O. Franck, A. M. Teale, and E. Fromager, *Mol. Phys.* **111**, 1275 (2013).
- [121] S. Vuckovic, T. J. Irons, A. Savin, A. M. Teale, and P. Gori-Giorgi, *J. Chem. Theory Comput.* **12**, 2598 (2016).
- [122] A. Görling and M. Levy, *Phys. Rev. B* **47**, 13105 (1993).
- [123] A. Görling and M. Levy, *Phys. Rev. A* **50**, 196 (1994).
- [124] R. R. Chasman, *Phys. Rev.* **138**, B326 (1965).
- [125] R. W. Richardson, *Phys. Rev.* **144**, 874 (1966).
- [126] R. W. Richardson, *Phys. Rev.* **154**, 1007 (1967).
- [127] G. K.-L. Chan and M. Head-Gordon, *J. Chem. Phys.* **116**, 4462 (2002).
- [128] G. K.-L. Chan, *J. Chem. Phys.* **120**, 3172 (2004).
- [129] D. Ghosh, J. Hachmann, T. Yanai, and G. K.-L. Chan, *J. Chem. Phys.* **128**, 144117 (2008).
- [130] S. Sharma and G. K.-L. Chan, *J. Chem. Phys.* **136**, 124121 (2012).
- [131] R. Olivares-Amaya, W. Hu, N. Nakatani, S. Sharma, J. Yang, and G. K.-L. Chan, *J. Chem. Phys.* **142**,

- 034102 (2015).
- [132] S. Guo, M. A. Watson, W. Hu, Q. Sun, and G. K.-L. Chan, *J. Chem. Theory Comput.* **12**, 1583 (2016).
- [133] L. M. Mentel, X. W. Sheng, O. V. Gritsenko, and E. J. Baerends, *J. Chem. Phys.* **137**, 204117 (2012).
- [134] F. Aquilante, J. Autschbach, R. K. Carlson, L. F. Chibotaru, M. G. Delcey, L. De Vico, I. Fdez. Galván, N. Ferré, L. M. Frutos, L. Gagliardi, *et al.*, “*Molcas 8: New capabilities for multiconfigurational quantum chemical calculations across the periodic table*,” (2016).
- [135] D. G. A. Smith, L. A. Burns, A. C. Simmonett, R. M. Parrish, M. C. Schieber, R. Galvelis, P. Kraus, H. Kruse, R. Di Remigio, A. Alenaizan, A. M. James, S. Lehtola, J. P. Misiewicz, M. Scheurer, R. A. Shaw, J. B. Schriber, Y. Xie, Z. L. Glick, D. A. Sirianni, J. S. O’Brien, J. M. Waldrop, A. Kumar, E. G. Hohenstein, B. P. Pritchard, B. R. Brooks, H. F. Schaefer, A. Y. Sokolov, K. Patkowski, A. E. DePrince, U. Bozkaya, R. A. King, F. A. Evangelista, J. M. Turney, T. D. Crawford, and C. D. Sherrill, *J. Chem. Phys.* **152**, 184108 (2020).
- [136] J. R. McClean, N. C. Rubin, K. J. Sung, I. D. Kivlichan, X. Bonet-Monroig, Y. Cao, C. Dai, E. S. Fried, C. Gidney, B. Gimby, P. Gokhale, T. Häner, T. Hardikar, V. Havlíček, O. Higgott, C. Huang, J. Izaac, Z. Jiang, X. Liu, S. McArdle, M. Neeley, T. O’Brien, B. O’Gorman, I. Ozfidan, M. D. Radin, J. Romero, N. P. D. Sawaya, B. Senjean, K. Setia, S. Sim, D. S. Steiger, M. Steudtner, Q. Sun, W. Sun, D. Wang, F. Zhang, and R. Babbush, *Quantum Sci. Technol.* **5**, 034014 (2020).
- [137] R. van Meer, O. V. Gritsenko, and E. J. Baerends, *J. Chem. Phys.* **148**, 104102 (2018).
- [138] P. A. Johnson, C.-É. Fecteau, F. Berthiaume, S. Cloutier, L. Carrier, M. Gratton, P. Bultinck, S. De Baerdemacker, D. Van Neck, P. Limacher, *et al.*, *J. Chem. Phys.* **153**, 104110 (2020).
- [139] K. Pernal, *Comput. Theor. Chem.* **1003**, 127 (2013).
- [140] I. A. Elayan, R. Gupta, and J. W. Hollett, *J. Chem. Phys.* **156**, 094102 (2022).
- [141] R. Gebauer, M. H. Cohen, and R. Car, *arXiv:1309.3929* (2013).
- [142] K. Head-Marsden and D. A. Mazziotti, *J. Phys. Chem. A* **124**, 4848 (2020).
- [143] D. R. Alcoba, O. B. Oña, L. Lain, A. Torre, P. Capuzzi, G. E. Massaccesi, E. Ríos, A. Rubio-García, and J. Dukelsky, *J. Chem. Phys.* **154**, 224104 (2021).
- [144] R. R. Li, M. D. Liebenthal, and A. E. DePrince III, *J. Chem. Phys.* **155**, 174110 (2021).
- [145] J. J. Shepherd, T. M. Henderson, and G. E. Scuseria, *J. Chem. Phys.* **144**, 094112 (2016).
- [146] C.-É. Fecteau, S. Cloutier, J.-D. Moisset, J. Boulay, P. Bultinck, A. Faribault, and P. A. Johnson, *arXiv:2202.12402* (2022).
- [147] V. E. Elfving, M. Millaruelo, J. A. Gámez, and C. Gogolin, *Phys. Rev. A* **103**, 032605 (2021).
- [148] M. Seidl, J. P. Perdew, and M. Levy, *Phys. Rev. A* **59**, 51 (1999).
- [149] M. Seidl, *Phys. Rev. A* **60**, 4387 (1999).
- [150] M. Seidl, J. P. Perdew, and S. Kurth, *Phys. Rev. Lett.* **84**, 5070 (2000).
- [151] M. Ernzerhof, *Chem. Phys. Lett.* **263**, 499 (1996).
- [152] P. Mori-Sánchez, A. J. Cohen, and W. Yang, *J. Chem. Phys.* **124**, 091102 (2006).
- [153] E. Fromager and H. J. Aa. Jensen, *Phys. Rev. A* **78**, 022504 (2008).
- [154] J. G. Ángyán, *Phys. Rev. A* **78**, 022510 (2008).
- [155] E. Fromager and H. J. Aa. Jensen, *J. Chem. Phys.* **135**, 034116 (2011).